Published in final edited form as:
J Vis. 2012 ; 12(4): . doi:10.1167/12.4.13.

Ocular following in humans: Spatial properties

Christian Quaia,
Laboratory of Sensorimotor Research, National Eye Institute, Bethesda, MD, USA

Boris M. Sheliga,
Laboratory of Sensorimotor Research, National Eye Institute, Bethesda, MD, USA

Edmond J. FitzGibbon, and
Laboratory of Sensorimotor Research, National Eye Institute, Bethesda, MD, USA

Lance M. Optican
Laboratory of Sensorimotor Research, National Eye Institute, Bethesda, MD, USA

Abstract

Ocular following responses (OFRs) are tracking eye movements elicited at ultrashort latency by the sudden movement of a textured pattern. Here we report the results of our study of their dependency on the spatial arrangement of the motion stimulus. Unlike previous studies that looked at the effect of stimulus size, we investigated the impact of stimulus location and how two distinct stimuli, presented together, collectively determine the OFR. We used as stimuli vertical gratings that moved in the horizontal direction and that were confined to either one or two 0.58° high strips, spanning the width of the screen. We found that the response to individual strips varied as a function of the location and spatial frequency (SF) of the stimulus. The response decreased as the stimulus eccentricity increased, but this relationship was more accentuated at high than at low spatial frequencies. We also found that when pairs of stimuli were presented, nearby stimuli interacted strongly, so that the response to the pair was barely larger than the response to a single strip in the pair. This suppressive effect faded away as the separation between the strips increased. The variation of the suppressive interaction with strip separation, paired with the dependency on eccentricity of the responses to single strips, caused the peak response for strip pairs to be achieved at a specific separation, which varied as a function of SF.

Keywords

ocular following; spatial frequency; stimulus

Introduction

Ocular following responses (OFRs) are reflexive, short-latency, tracking eye movements elicited by the sudden movement of a textured pattern (Masson & Perrinet, 2012; Miles, 1998; Miles & Sheliga, 2010). They are elicited by the type of laminar flow that a subject experiences as he/she moves in one direction and looks off to one side. It has thus been proposed that the ocular following system evolved to supplement the translational VOR system, helping in the stabilization of gaze. In initial studies (Miles, Kawano, & Optican, 1986), large-field stimuli were found to be very effective at inducing robust OFRs, and thus,

Corresponding author: Christian Quaia, Address: National Eye Institute, 49 Convert Dr, Rm 2A50, Bethesda, MD 20815, USA, quaiac@nei.nih.gov.

Commercial relationships: none.

the ocular following system has been largely characterized using such stimuli (with coverage ranging from a *ganzfeld* down to the central 30°).

When tested with sinusoidal gratings, the OFRs are tuned, in a close to separable manner, for spatial and temporal frequencies (Gellman, Carl, & Miles, 1990; Miles et al., 1986). In a sense, this is quite an unexpected result: Since ocular following is a tracking system, one would expect the speed of the eyes to be determined by the speed of the stimulus (the ratio of temporal and spatial frequencies), but this is not the case. Similarly, changes in the spatial extent of the stimulus (diameter of a disk) have been shown (Barthelemy, Vanzetta, & Masson, 2006) to result in OFR changes, in spite of a constant stimulus speed. Such an apparently suboptimal behavior is probably related to the ultrashort latency of these movements: Not much time is available to perform complex calculations, so that the OFRs primarily reflect the feed-forward processing of early cortical visual areas (Masson & Perrinet, 2012; Miles, 1998; Miles & Sheliga, 2010). Accordingly, in recent years OFRs have been used as a powerful probe for investigating visual processes.

Recent studies (Barthelemy et al., 2006; Sheliga, Fitzgibbon, & Miles, 2008a; Sheliga, FitzGibbon, & Miles, 2008b) have revealed that whereas large stimuli induce strong OFRs, much smaller coverage areas are in fact sufficient to produce reliably measurable OFRs. In particular, Sheliga et al. (2008a, 2008b) have shown that the rapid motion of vertical sine-wave gratings presented in strips only 1° high induces horizontal OFRs at the typical short latencies. This recent development adds a new dimension to the applicability of the OFR as a probe for the visual system: Properties that vary as a function of the location of a stimulus on the retina, or interactions between multiple stimuli present in the visual field, have become amenable to OFR-based investigations.

Here we report the results of our exploration, in human subjects, of the effect that the spatial arrangement of the visual stimulus has on the OFRs. We reasoned that it would be particularly interesting to know (1) how the OFR varies as a function of the spatial location of the stimulus and (2) how two simultaneously presented stimuli, differing only in their spatial location, interact. These two properties represent the cornerstone of all models of spatial summation, whether they attempt to reproduce the characteristics of receptive fields of visual neurons or perceptual behavior. Studying how the OFRs are affected under these circumstances could provide us with a window into the workings of visual motion processing areas.

We thus measured responses to the smallest stimuli that were sufficient to induce reliable short-latency OFRs over a large part of the visual field. An initial pilot study (our unpublished observations) revealed that 0.5° high strips, spanning the width of the screen, represented a lower limit, guaranteeing an acceptable signal-to-noise ratio in most subjects. Note that the conditions that we test in this study are much simpler than those of earlier studies showing that OFRs are not tuned for the speed of the stimulus. Unlike the conditions that led to the temporal frequency/speed dichotomy, here we look at identical stimuli (same spatial frequency, temporal frequency, motion direction, and extent), which only differ in their spatial location. Similarly, to study potential interactions among stimuli, we look not at the responses induced by stimuli of different sizes but rather at how the response to a pair of stimuli (again, differing only in spatial location) compares to the responses to the individual stimuli, as a function of the separation between the stimuli.

If the ocular following system were to behave as a tracking mechanism under these conditions, we would expect the OFRs to individual stimuli to be independent of their location. We report instead that dramatic variations are observed, more so for high than for low spatial frequencies. This reinforces the idea that OFRs arise from very basic filtering

operations on the motion stimulus, lacking the sophistication that would be required for a full-blown tracking system. It appears that, with our elemental stimuli, the OFR magnitude varies with eccentricity as contrast sensitivity does (Banks, Sekuler, & Anderson, 1991; Foley, Varadharajan, Koh, & Farias, 2007; Pointer & Hess, 1989; Robson & Graham, 1981). This relationship largely mirrors the spatial distribution of photoreceptors in the retina and neural receptive fields (RFs) in visual areas. Moreover, when two stimuli, placed symmetrically about center gaze, and thus eliciting by themselves very similar responses, are displayed simultaneously, they interact in a complex manner. The strength of this interaction is modulated by the distance between the strips, by the width of the strips, by the spatial frequency of the gratings, and, to a smaller extent, by their contrast.

Methods

Subjects

Three subjects participated in the experiment, all authors (note that the eye movements reported here are reflexive and have an ultrashort latency, so that they occur well before the subject could react to the stimulus). All had normal or corrected-to-normal visual acuity. All had previous experience with wearing search coils. Experimental protocols were approved by the Institutional Review Board concerned with the use of human subjects.

Visual apparatus

The subjects sat in a dark room and were positioned so that their eyes were located approximately in the center of a cubic box (70 cm side) containing orthogonal magnetic field generating coils. Their chin and forehead rested on padded supports, and their head was stabilized using a headband. Visual stimuli were presented on a CRT monitor located straight ahead 460 mm from the corneal vertex. The monitor screen was 400 mm wide (corresponding to 47° of visual angle) by 300 mm high (corresponding to 36° of visual angle), and its resolution was 1024 by 768 pixels. We actually used two similar monitors, one (Sony GDM-C520) with a vertical refresh rate of 150 Hz and the other (Sony GDM-F520) with a rate of 160 Hz. The background luminance was set to 20.8 cd/m^2 (as reported by a Konica Minolta LS100 luminance meter). The RGB signals from the video card (NVIDIA Quadro FX 5600) provided the inputs to an attenuator whose output was connected to a single channel of a video signal splitter (Black Box, AC085A-R2); the video outputs of the splitter were then connected to the RGB inputs of the monitor. In this way, only grayscale images could be presented but with a higher luminance resolution (theoretically 12 bits) than normally possible (8 bits). Luminance linearization (typically, $r^2 > 0.99997$) was performed by interpolation following dense luminance sampling.

Eye movement recording

A scleral search coil embedded in a silastin ring (Skalar; Collewijn, van der Mark, & Jansen, 1975) was placed in each subject's dominant eye following application of topical anesthetic (proparacaine HCl). The horizontal and vertical orientations of the eye were recorded using an electromagnetic induction technique (Robinson, 1963). The AC voltages induced in the coil were processed by phase-locked amplifiers (CNC Engineering), providing separate DC voltages proportional to the horizontal and vertical orientations of the eye. These outputs were calibrated at the beginning of each recording session using a two-step procedure. First, the subjects were asked to look at one of five targets (straight ahead or 10° along each cardinal direction), while the experimenter adjusted the gain and bias of the coil amplifiers. This allowed, to a first-order approximation, the coil signals to be brought into register with the experiment control software, which is necessary to impose an online fixation window. Subsequently, subjects had to fixate a target that appeared at ±5° of eccentricity (horizontal or vertical) and press a button when they were confident that they were accurately foveating.

This procedure was repeated four times for each target, and the data collected were used offline to linearize the coil signals recorded during the experiments (by fitting with second-order polynomials). Peak-to-peak noise levels resulted in an uncertainty in eye position recording of less than 0.03° in either setup. Coil signals were sampled at 1000 Hz.

Experiment control

The experiment was controlled by two computers, communicating over an ethernet with TCP/IP. The Real-time EXperimentation software package (Hays, Richmond, & Optican, 1982), running on the master computer under the QNX operating system, was responsible for providing the overall experimental control as well as acquiring, displaying, and storing the eye movement data. Another machine, directly connected to the CRT display, generated the required visual stimuli in response to REX commands. This was accomplished using the Psychophysics Toolbox v. 3.0.8 and a set of Matlab (Mathworks, MA) scripts and functions (Brainard, 1997; Pelli, 1997).

Visual stimuli and paradigm

In all experiments, the visual stimuli were 1D vertical gratings with sinusoidal luminance profiles. The average luminance of the grating was equal to the luminance of the background (20.8 cd/m^2). Unless otherwise noted, the stimulus' Michelson contrast (Michelson, 1927) was 32%.

Because the front-end of the visual system performs a filtering operation that can be loosely described as a localized 2D Fourier decomposition of its input (Daugman, 1980, 1984; Pollen & Ronner, 1983), carrying out a high-resolution experiment in space and spatial frequency is not simple. The problem is that the more localized a stimulus is in space, the less localized it is in the Fourier domain (Bracewell, 2003; Daugman, 1985), inevitably introducing a trade-off in any experimental design. So, for example, if a grating within a circular window were used as a stimulus, shrinking the diameter of the window would cause the 2D Fourier representation of the stimulus to spread out from the spatial frequency and orientation of the grating. Using very small stimuli is thus dangerous, as it inevitably leads to poor resolution in Fourier space. Using small widths (e.g., less than a grating cycle) is particularly dangerous in motion experiments, as the increased bandwidth includes higher harmonics that, because of aliasing, can actually move in the direction opposite that of the stimulus (Anderson & Burr, 1991). Conversely, with large stimuli the spatial resolution is low. In the context of our experiments, using strips with a large width (i.e., as many cycles of the grating as possible) and a small height represented an ideal trade-off, allowing us to maintain a high resolution for spatial frequency, while covering a relatively small area. The downside is that neurons tuned to a fairly wide range of orientations (around the orientation of the grating) were probably activated, but orientation resolution is not something we were interested in. Accordingly, in most of our experiments the gratings extended the full width of the display.

The stimuli occupied either a single strip, approximately 0.58° high, or two such strips. Because of the granularity of the display, it was not possible to present a strip subtending the same visual angle at all elevations. Thus, we chose the integer number of pixels that resulted in a strip height as close as possible to 0.58° (12 pixels in the center, 13 in the far periphery). At the edge of the strip, the transition between the grating and the background was abrupt (i.e., there was no smooth contrast transition). The spatial frequency of the grating stimulus was adjusted to take into account the magnification factor of the corrective lenses worn by each subject. However, the SF was not adjusted for eccentricity: As has been traditionally done in ocular following experiments, the stimuli were pure sinusoids on the screen, not on

the retina. Accordingly, the local SF is actually equal to the nominal SF multiplied by [1 + $\tan^2$ (ecc)]. At the edge of the screen, the SF is thus 18% higher than in the center.

Trials were presented in blocks; each block contained one trial for each stimulus condition. All conditions within a block were randomly interleaved. Each trial began with the appearance of a central fixation point, having a diameter of 0.2° of visual angle, superimposed on a static grating stimulus. The fixation point was either light gray with a very small dark gray dot in its center or dark gray with a very small light gray dot in its center. The two were alternated across trials, to reduce potential aftereffects. The luminances used were 60 cd/m^2 and 0.1 cd/m^2, larger than the maximum, and smaller than the minimum, used in the stimuli. This ensured that the FP was always clearly visible, even when it was superimposed on a high-contrast grating. The subject was instructed to look at the fixation point and avoid making saccadic eye movements. After the subject maintained fixation within a small (1° on the side) invisible window around the fixation point for 500–700 ms, the fixation point disappeared, and simultaneously apparent motion (either leftward or rightward, equally likely and randomly selected) of the grating was induced by sequentially shifting it by one eighth of its wavelength at each frame. The temporal frequency of the stimulus was thus 18.75 Hz with one monitor and 20 Hz with the other, corresponding to the region of maximum OFR sensitivity in humans (Gellman et al., 1990). The motion lasted for approximately 200 ms, after which the whole screen turned gray (again at 20.8 cd/m^2), signaling the end of the trial. After a short intertrial interval, adjusted according to each subject's preference, a new trial was started. If the subject blinked, or if saccades were detected during the motion epoch, the trial was discarded and repeated within the block. The number of blocks acquired within each experiment varied from subject to subject, depending on each subject's signal-to-noise ratio. With few exceptions, a single experiment required multiple daily recording sessions to collect enough trials from a subject (we collected between 100 and 150 trials for each condition and between 1500 and 3000 trials in a session; the number of conditions varied across experiments).

Data analysis

The calibrated eye position traces (see Eye movement recording section) were smoothed with a non-causal (zero delay) 6th-order Butterworth filter (3 dB at 30 Hz), and eye-velocity traces were computed using a Savitzky–Golay filter (Savitzky & Golay, 1964; 4th-order polynomial, kernel size of 11). Average temporal profiles time-locked to stimulus onset were computed separately for each stimulus condition. Trials with saccadic intrusions that went undetected at run time were manually removed.

To benefit from a higher signal-to-noise ratio, most ocular following studies report not the raw OFR but rather the difference between the OFRs to rightward and leftward motion. We did so too. In our study, adopting this measure carries benefits beyond that of improving the signal quality. Since our analysis of the interaction between stimuli relies heavily on comparisons between the magnitude of OFRs to different stimuli, it would be greatly impacted by the potential presence of an OFR component that is triggered by the motion stimulus but that is independent of its spatiotemporal properties, including its direction (i.e., it is not stimulus selective). We have in fact found strong evidence to support the presence of such a *default response* (see Appendix A). By basing our OFR measurements on the difference between the eye velocity induced by the same stimulus moving in opposite directions (Figure 1), we cancel any possible contribution of this spurious component.

OFR responses are usually characterized by two measures: latency and magnitude. With more complex stimuli, the time evolution of the response can be highly informative (Gellman et al., 1990; Masson & Castet, 2002; Masson, Rybarczyk, Castet, & Mestre, 2000; Miles et al., 1986), but with our simple stimuli we did not find any obvious time-dependent

effects. In general, latencies and magnitudes were negatively correlated, so that weaker responses were delayed compared to stronger ones. This was true whether the difference in strength was related to stimulus eccentricity or width. Just as reported in earlier studies, much larger latency differences were observed when contrast was varied. Accordingly, we do not present separate analyses on the latency of the OFRs measured in this study.

Whereas latency is an intuitive concept (although it is often difficult to define a robust procedure to quantify it), defining the magnitude of the OFR is less straightforward. We, like others before us, defined it as the average eye speed in a time window, but there is no inherently "correct" way of selecting the window. The only hard constraint is that the window must be wholly contained within the open-loop period of the response (i.e., the time period between response onset and twice the response latency). There are then essentially two principled ways of selecting the window. The first one (*stimulus-based*) uses a fixed window for all stimuli whose responses are compared, time-locked to the stimulus onset. The second one (*response-based*) entails using a window that starts at the latency of each response. In both cases, a constant window duration must be used, equal to, or shorter than, the shortest latency. In some of our analyses, we directly compared the response to a pair of strips to those induced by the individual strips in the pair; obviously using measures computed over different time windows would be hard to justify. Accordingly, we defined an additional *pair-based* measure, i.e., a measure such that responses to the two individual strips that make up a pair, and to the pair itself, are computed using the same window. Since the OFR to the pair was typically more robust than that to the individual strips, its latency was used to define the pair-based time window. Because no measure can be said to be unequivocally superior, we performed all the analyses presented here twice, once with the stimulus-based measures and once with the pair-based measures. We generally report the results based on the stimulus-based measures but also point out if and how pair-based measures differed. When we describe the responses to individual strips, we also refer to the response-based measure, since in that case a pair-based measure would not make sense.

Statistical analysis

As mentioned above, almost all the measures reported herein are in fact differences between two sets of independent measurements (responses to the same stimulus moving in opposite directions). Because of the small number of trials that had to be excluded post-hoc for saccadic intrusions, the number of useable trials for the two measurements to be subtracted was usually not identical. Under these circumstances, some care must be applied to correctly analyze the data, even if the noise in the data is independent and normally distributed. It is generally accepted that in these cases the safest approach is to use resampling methods (Efron, 1982). Accordingly, we have used bootstrap-based methods for almost all of our statistical analyses. Here we briefly describe the procedures used for each measure.

First, we quantified the measure of interest in individual trials by computing, for each trial, the average eye speed S in a time window (see above). To compute the OFR associated with a stimulus, we then considered, separately for each stimulus, the N_L trials ($\mathbf{S}_L$ being the vector of their S measures) associated with leftward motion and the N_R trials ($\mathbf{S}_R$) associated with rightward motion. The difference between the mean measure for rightward and leftward trials $M = \Sigma_i S_{Ri}/N_R - \Sigma_j S_{Lj}/N_L$ is the mean value of our measure. To obtain a confidence interval around M, we then selected, with replacement, N_L trials from $\mathbf{S}_L$ and N_R trials from $\mathbf{S}_R$ and computed the difference of their means. This was repeated 1000 times, producing a distribution of bootstrapped means $\mathbf{M}^*$. Since the distribution was always Gaussian with mean M, for plotting purposes we used its standard deviation as the standard error of the mean value M (SEM). The same type of procedure can be used to compute not

just the difference but any function of unpaired measures (such as the mean or ratio of two measures).

Once we have a distribution of bootstrapped means for each of our OFR measures, it is rather easy to test whether two such means are significantly different. All that is needed is to repeatedly sample one value from each distribution and subtract them (or even simply subtract the values from the two distributions in the order they were generated) and verify whether the 95% confidence interval (i.e., from its 2.5 to its 97.5 percentile) of the distribution of differences straddles zero. The smallest among the fraction of differences that are above and below zero, multiplied by two, is equivalent to the *p*-value returned by a two-tailed unpaired *t* test (Simon, 1995).

On two occasions, we were interested in testing whether there was a trend across conditions, i.e., whether the mean across a set A of conditions was different than the mean across another set B of conditions. For each set, we created a distribution of means by computing, repeatedly, the average of samples obtained by picking one sample from the **M*** distribution for each of the conditions belonging to the set. The difference between the distributions of set means for each set was then computed as above.

Similar principles were applied to curve fitting. To compute confidence intervals on the parameters of the fit to a set of conditions, we computed a distribution of fits by selecting, 1000 times, single samples from the **M*** distribution for each of the conditions belonging to the set and fitting a curve to it. From this distribution of fit parameters, we could then extract the mean and *SEM* for any of the parameters (either from the mean and standard deviation of the distribution, if, based on the Jarque–Bera test, it could be considered normally distributed or as its median and 68% confidence interval if it could not). Testing for significant differences between parameters of two curves fit to different sets of conditions could then be carried out as mentioned above, by verifying whether the 95% confidence interval of the distribution of differences straddled zero.

Results

We measured the OFR to horizontal strips (0.58° high) containing a vertical sinusoidal grating. In our main experiment, the stimuli were either a single strip located at one of 17 different elevations (centered at eye level, ±0.3°, ±0.6°, ±1.2°, ±2.3°, ±4.7°, ±9.3°, ±13.7°, and ±17.5°) or two of the single strips located symmetrically about eye level. Note that, because of the locations chosen, the pair with the closest strips actually appeared as a single strip, 1.16° high, centered at eye level. Response to both leftward and rightward motion was measured, with all conditions randomly intermixed. The measures reported herein are based on the difference between the response to rightward and leftward motion (see Data analysis section).

Effect of stimulus location

The first goal of our study was to quantify the dependency of the OFR on the eccentricity of the stimulus and to determine how this relationship varies with the spatial frequency (SF) of the stimulus. It is important to note that because our stimuli were wide strips when we use the term eccentricity we actually refer to the elevation of the strip, i.e., the minimum eccentricity of the stimulus. Accordingly, low eccentricity stimuli actually stimulate both central and peripheral regions of the retina, and as the eccentricity is increased, the region stimulated shifts toward the peripheral retina.

We presented, at one of 17 vertical eccentricities (elevations), a horizontal strip containing a vertical sinusoidal grating having one of three SFs. In all subjects, we tested the SF that

generates the strongest response (0.25 cpd) and two flanking frequencies. In subjects BMS and EJF, we used flanking frequencies that were three times and one third of the preferred SF. Because of the small size of CQ's responses, in that subject we used instead SFs that were twice and one half of the preferred SF.

First, we tested whether there were systematic differences between the responses to single strips located symmetrically either above or below eye level. According to the psychophysics literature, a difference could be expected, more accentuated as the stimuli are moved toward the periphery. Our findings were quite inconsistent across subjects and spatial frequencies. In subject BMS, we found a significant effect ($p < 0.05$, two-way univariate ANOVA, with eccentricity and up vs. down elevation as factors, separately for leftward and rightward motion) only at high SF, with stimuli above eye level producing slightly stronger responses than stimuli below eye level. For low and intermediate SFs, the test revealed no significant differences. In subject CQ, there were no significant differences at any of the three SFs tested. In subject EJF, there were instead significant effects at all frequencies, with stimuli below eye level producing stronger responses than stimuli above eye level (i.e., in the opposite direction as the effect found in BMS). This difference increased with eccentricity, from 0.06°/s at the smallest eccentricities to 0.16°/s at the largest eccentricity (average across SFs in subject EJF).

The general relationship between OFR and eccentricity was however the same above and below eye level in all three subjects. Accordingly, in Figure 2 we plot, as a function of eccentricity, the average OFR elicited by stimuli equidistant from eye level. While there were some quantitative differences across subjects, qualitatively the subjects behaved similarly. The responses decreased as the eccentricity of the strip increased, more so for high than for low spatial frequencies. This behavior was virtually identical when response-based measures (i.e., the measurement time window starts at response onset; see Methods section) were used. We interpret these results as being broadly compatible with the known distribution of receptive fields (RFs) in primary visual cortex. RFs tuned to high SFs are more abundant in the center than in the periphery, so that as the stimulus is moved away from the center the central RFs that lose stimulation outnumber the peripheral RFs that gain it. RFs tuned to low SFs are more evenly distributed across visual space, so that the effect of moving the stimulus to larger eccentricities is less severe.

Integration over two stimuli

The second stimulus type that we used in our main experiment was a pair of strips, placed symmetrically above and below eye level. The responses to these stimuli (Figure 3) were qualitatively similar to those to single strips, in the sense that central strips induced stronger responses than peripheral strips. There was however also a major difference: The responses to the pairs did not peak for the smallest separation (i.e., a large strip at eye level), as would be expected if the effects of individual strips simply summed. Instead, the peak response to pairs of strips was elicited when the two strips were separated, and the distance associated with the peak response varied as a function of SF. At high SFs, the peak was reached for relatively close together strips, but this distance increased as the SF decreased.

We suspected that the separation associated with the peak response (in short, peak separation) might reveal something fundamental about the spatial summation properties of visual neurons. To further investigate this issue, we thus tested, in two subjects, how the peak location varies over a wider range of SFs (0.03 cpd ≤ SF ≤ 2.0 cpd). In this experiment, only pairs of strips were used as stimuli (no single strips were presented). The relationship between strip separation and OFR was then estimated, separately for each SF, using a polynomial fit; peak separation was defined as the location of the peak of the polynomial curve. Confidence intervals for the peak separation were found by repeating the operation in

the context of a bootstrap procedure (see Methods section). Very low SFs (SF < 0.125 cpd) were discarded because the OFRs modulated little with separation, so that the location of the peak was poorly constrained. Furthermore, the absolute location of the peak varied depending on the order of the fitting polynomial and on whether the fit was performed on a linear or on a logarithmic separation scale. We thus computed the peak separation for three polynomial orders (2, 3, and 4) and on both linear and logarithmic response scales. We found that in all cases the peak separation decreased with increasing SF. In Figure 4, we plot, for both subjects, the relationship obtained using a third-order polynomial, with the fit applied either to the relationship between OFR and separation (linear) or to that between OFR and the logarithm of the separation (log). In all cases, the OFRs in subject BMS peaked at slightly larger separations that those in subject EJF (also apparent from Figure 3). Furthermore, the fits in linear coordinates yielded peaks at larger eccentricities than those in log coordinates, especially at low SFs. The qualitative relationship between peak separation and SF (here fitted with a decaying exponential) was however very robust and highly consistent.

Interaction between stimuli

A qualitative comparison between the responses to single strips and strip pairs reveals a non-linear interaction between the two strips. To quantify this interaction, we thus computed the following interaction index:

$$I_I = \frac{\mathrm{OFR}(A+B)}{\mathrm{OFR}(A)+\mathrm{OFR}(B)} = \frac{\mathrm{OFR}_{\mathrm{PAIR}}}{\sum \mathrm{OFR}_{\mathrm{SINGLE}}}. \quad (1)$$

A value of 1.0 would indicate that the two strips do not interact and that the OFR to the pair is equal to the sum of the OFRs to the individual strips. In other words, the ocular following system would obey linear spatial summation. Values lower than 1.0 indicate a suppressive interaction, whereas values larger than 1.0 indicate facilitation. Since, as noted above, the OFR to the individual strips in a pair (located at the same distance from eye level) is approximately the same, a value of 0.5 would essentially indicate that the system responds just as strongly to a single strip and to the pair (averaging).

In Figure 5 (top row), we plot the relationship between the interaction index and the separation between the strips, separately for each subject and SF tested. The data points (mean ± *SEM*; see Methods section) are plotted, together with an exponential function fitted by weighted least squares to the data. We found that when the strips were close together there was, for all SFs tested, a very strong suppression, with an interaction index as low as 0.5; as the separation between strips increased, I_I increased as well. While this overall pattern is highly consistent across subjects, at large separations the results are much less consistent. In particular, we found that in some conditions the I_I can be significantly larger than 1.0, indicating a facilitatory interaction.

There is however one issue that makes I_I, as computed so far, potentially unreliable at large separations: As noted in the Methods section, and as can be seen in Figure 1, when single strips at large eccentricities are presented the onset time of the response is delayed, occasionally by as much as 30 ms. Obviously, by using a time window that starts several milliseconds before the response onset we inevitably include noise, thus potentially reducing the S/N ratio. To evaluate the impact of this issue on our analysis, we computed a measure of the OFR that is based on a time window locked not to the onset of the stimulus but rather to the onset of the response to a pair of stimuli (pair-based response; see Methods section). The duration of the time window over which the average speed is computed is kept the same, but it is shifted in time to match the response onset. When this pair-based analysis on

the differential OFRs is performed (Figure 5, bottom row), some of the I_I values do change somewhat, mostly at high SF, and the error bars for larger separations are moderately reduced. However, the overall behavior is unchanged, and the facilitatory interaction between distant stimuli is still present.

In the above analysis, we have uncritically assumed that the separation between strips is what determines I_I. There are however some potential alternative interpretations. First, we have shown that as the eccentricity of a strip increases, the magnitude of the OFR it induces decreases (Figure 2). It could then be argued that what determines I_I is not the separation between the two strips (a sensory property) but rather the magnitude of the OFRs that they induce (a motor property). Second, it is not clear what role, if any, the non-Fourier (or second-order) motion signals present at the long edges of our stimuli might play in determining our responses.

We have tested these hypotheses in a series of control experiments, which are described in Appendix B. These experiments allowed us to conclude that: (1) the major determinant of I_I is the separation between strips, and response magnitude plays a small or no role (the interactions are thus determined by sensory, not motor, processes); and 2) all our conclusions apply to first-order motion and are not affected by any second-order motion artifact.

Effect of contrast

In all the experiments described so far, the stimuli had a Michelson contrast of 32%, which is known to elicit maximal, or close to maximal, OFRs, at least with large stimuli (Miles et al., 1986; Sheliga, Chen, Fitzgibbon, & Miles, 2005). Since it is also known that contrast affects OFRs by modulating their latency and magnitude (Barthelemy et al., 2006; Miles et al., 1986; Sheliga et al., 2005), it would be interesting to know whether contrast affects the response to our stimuli and, in particular, whether the interaction between two stimuli is affected by contrast. This is particularly important since it has been firmly established that, in spite of the presence of several contrast normalization mechanisms along the visual pathway, stimulus contrast plays a prominent role in determining the response of neurons in visual cortex, modulating not just the latency and magnitude of their response but also altering the spatiotemporal properties of their receptive fields (Cavanaugh, Bair, & Movshon, 2002; Kapadia, Westheimer, & Gilbert, 1999; Kohn & Smith, 2005; Levitt & Lund, 1997; Nauhaus, Busse, Carandini, & Ringach, 2009; Polat, Mizobe, Pettet, Kasamatsu, & Norcia, 1998; Sceniak, Ringach, Hawken, & Shapley, 1999).

Because the contrast response curve for small strips like ours has not been measured before, we started by determining, in two subjects, how the OFR elicited by individual strips changes as a function of contrast. We presented a strip either centrally (±0.3°) or more peripherally (±9.3°) and varied the Michelson contrast of the grating between 3% and 96%, in octave increments. Since responses would be reduced at lower contrast, to obtain an acceptable S/N ratio we focused on the best SF. We fitted the contrast response curves using the generalized Michaelis–Menten (also referred to as the Naka–Rushton) curve:

$$R = R_{\max} \frac{c^n}{c^n + c_{50}^n}. \quad (2)$$

In Figure 6, we plot the OFRs together with fits for both subjects. Note that we used stimulus-based measures, i.e., even though the latency increased considerably as contrast decreased (from 66 ms to 102 ms in subject BMS and from 62 ms to 96 ms in subject CQ), for all stimuli we used the same measuring time window (within a subject), starting from the

latency of the response to the highest contrast stimulus. In the top panels, raw measures are shown, whereas the bottom panels show responses that have been normalized based on the value of R_{max}. To evaluate the fits statistically, we used a bootstrap procedure (see Methods section). The semi-saturation constant was around 11%: for the central strip, which has a better S/N ratio, median c_{50} was 10.9% (68% CI = 9.7%–12.5%) for BMS and 12.0% (68% CI = 10.6%–14.2%) for CQ. The exponent n had a median value of 1.22 (68% CI = 1.09–1.36) for BMS and 1.80 (68% CI = 1.48–2.20) for CQ. For the peripheral strip, median c_{50} was 10.4% (68% CI = 9.4%–11.6%) for BMS and 16.2% (68% CI = 11.7%–22.8%) for CQ. The exponent n had a median value of 1.52 (68% CI = 1.36–1.70) for BMS and 2.19 (68% CI = 1.59–3.50) for CQ. Besides the obvious difference in R_{max} ($p < 0.01$; see Methods section), the contrast response curves were remarkably similar at the two eccentricities tested. In both subjects, n and c_{50} were not significantly different ($p > 0.15$ in all cases). An obvious effect of eccentricity was that at the lowest contrasts (3% in BMS and 3% and 6% in CQ) the response to the peripheral strips was attenuated more than would be expected from the attenuation at higher contrasts. In particular, subject CQ did not respond at all, regardless of the measuring time window used, to the peripheral 3% contrast stimulus (which was at the detection threshold).

Based on this experiment, we decided to directly compare the responses to single strips and strip pairs at two contrast levels: 8% (just below c_{50}) and 64% (at saturation). In Figure 7, we plot the results of this experiment, in our three subjects (SF was always 0.25 cpd). Note that the range of separations used was smaller than in our main experiment. In the top panels, we plot the responses to the strip pairs. The responses to the low-contrast stimuli (OFRs to pairs shown in the top panels) are essentially a scaled version of those to high-contrast stimuli, and the location of the peak response does not appear to be systematically affected by contrast. When the interaction index is considered (bottom panels), a consistent pattern emerges: at lower contrast, I_I is marginally larger, essentially at all separations. With the possible exception (depending on whether the Bonferroni correction for multiple comparisons is applied) of the smallest separation for subject EJF, pairwise comparisons are never significantly different ($p > 0.05$), but there is an overall trend. For BMS and EJF, the mean I_I was significantly larger ($p = 0.03$ and $p < 0.01$, respectively) at low contrast but not for CQ ($p = 0.09$). We take this to mean that as contrast was reduced the interaction index increased, albeit only slightly (on average by 0.09).

As noted above, the contrast response curves were all computed based on stimulus-based measures, as was done in previous ocular following studies. Since response latency increases as contrast decreases, this measure does not fit the intuitive definition of response magnitude. Indeed, when we computed the contrast response curves shown in Figure 6 using a response-based measure (i.e., the average speed in a time window that starts at response onset and thus is different for each stimulus), we found a much lower value for the semi-saturation contrast, with a median value for the more central stimuli of 2.65% in BMS (68% CI = 2.47%–2.81%) and 5.88% in CQ (68% CI = 5.29%–6.57%). The effect on the interaction index shown in Figure 7 is however not dependent on the type of measure used: With response-based measures, the interaction index shows the same, small, increase at the lower contrast. It could then be reasonably argued that the 8% contrast used above was not sufficiently low and that the small impact that such a large change in contrast had on the interaction index was simply a result of a very strong contrast normalization mechanism.

To better study the relationship between contrast and interaction index, we thus ran on two subjects an additional experiment, in which we used only two single strips, located at ±7° of eccentricity, and the corresponding pair but at six different contrasts (between 3% and 96%, in octave increments). Once again, subject CQ did not respond to the 3% contrast stimuli. In both subjects, we found that the interaction index increases somewhat as contrast decreased

(Figure 8, top row shows parameter computed using stimulus-based measures, and bottom row shows parameter computed using pair-based measures), but a sizeable effect of contrast is apparent only at extremely low contrasts. Unfortunately, at that point, the signal is so small that the uncertainty on the interaction index becomes very large. It would thus seem that the suppressive interactions might indeed weaken with contrast, but only at very low levels, around and just above the detection threshold. Obviously, it would be very hard to carry out a full experiment, like the one we described above at 8% contrast, at these contrast levels, since unveiling significant changes would require a very large number of trials per condition. In addition, working on the slope of such a steep contrast response curve would make the results extremely sensitive to contrast adaptation mechanisms, potentially leading to a non-stationary behavior.

Effect of strip width

In the experiments described so far, we used strips that spanned the entire screen (47°). Using wide strips has the advantage of tightly localizing the stimulus in frequency space, but it leaves open the question of how collinear stimuli interact to determine the OFR (i.e., summation along the axis of motion). In an attempt to at least partially address this issue, we conducted another experiment, in two subjects, in which we presented strips that spanned 8°, 16°, or 32°. Only the optimal SF (0.25 cpd) was used. Contrast was 32%, and the contrast transition at the ends of the grating (1 degree) was smoothed through cosine windowing. Because the narrower strips induced considerably smaller responses, we were also forced to restrict the eccentricity of the stimuli. In Figure 9, we plot the results of this experiment. The responses to single strips (leftmost column) show a small decrease over the limited range of eccentricities tested. The decrease was generally not significant ($p > 0.05$) with the exception of the widest strips in subject CQ ($p = 0.01$). For strip pairs, the responses instead increase over the range tested, with OFRs for 4° of separation significantly larger ($p < 0.001$ in all cases) than those induced at the smallest separation (0.6°, abutting strips). Obviously, the non-linear interactions that we have described for full-width stimuli are present even for the smaller stimuli. In general, the interaction index increased with separation, as seen for the full-width strips. However, this effect became more dramatic as the width of the strips decreased.

A simple model

The cascade of neural events that eventually leads to the OFRs that we measured involves a large number of areas (Masson & Perrinet, 2012). Obviously, based on the relatively small number of experiments that we have described here, it is impossible to attribute any of the properties we observed to any specific area or mechanism and to model them accordingly. Nevertheless, it would be desirable to put forward at least a simple model capable of reproducing the most salient aspects of the responses. Such a model would succinctly summarize our data, and it would be a step toward determining the behavioral receptive field for the ocular following system, as advocated by Barthelemy et al. (2006) and Masson and Perrinet (2012).

After experimenting with different architectures, we found that a very simple model could account reasonably well for our data. The model is composed of three layers of units, and it has no dynamics; its output is an estimate of the magnitude of the OFR. The first layer simply represents the inputs and, more precisely, a thin horizontal strip on the screen. Each unit subtends the same visual angle Δx_1 (vertical extent), and its output is 1.0 if the strip is occupied by a drifting vertical grating and 0.0 if it is not:

$$L_{1j}=\begin{cases} 0.0 & : \text{ No stim centered at } x_{1j} \\ 1.0 & : \text{ Stim centered at } x_{1j} \end{cases}. \quad (3)$$

Here x_{1j} is the center of the "receptive field" of the jth unit in the first layer. The second layer has many fewer units than the first one (i.e., larger "receptive fields"), and each unit computes a weighted sum of the outputs of the first layer. The weighting function is a Gaussian, with unitary height and coefficient of dispersion σ_e. All units in the second layer share the same σ_e, but they are shifted along the input layer, so that each unit in the second layer samples from a different subset of the first layer:

$$L_{2i}=\Delta x_1 \sum_j L_{1j} e^{-\frac{(x_{1j}-x_{2i})^2}{2\sigma_e^2}}. \quad (4)$$

Here x_{2i} is the center of the "receptive field" of the ith unit in the second layer. The third layer has the same number of units as the second layer and carries out a sort of global divisive normalization (Grossberg, 1973; Heeger, 1992) on the output of the second layer:

$$L_{3i}=\frac{\sqrt{L_{2i}}}{1.0+f(\sum_j L_{2j})}. \quad (5)$$

Here $f(\cdot)$ is a cumulative Gaussian function:

$$f(y)=\frac{1}{2}\left[1+\text{erf}\left(\frac{y-\mu_n}{\sqrt{2}\sigma_n}\right)\right], \quad (6)$$

with parameters μ_n and σ_n. Since $f(\cdot)$ varies between 0.0 and 1.0, the denominator in Equation 5 varies between 1.0 and 2.0. Note that it only assumes one of two values: one when one strip is presented and another when a pair is presented, regardless of strip location or separation. The outputs of the third layer are then summed. Since all the model elements are identical, changing the location of a stimulus would only change which units in the third layer are activated but not how strongly. To enable the model to account for the observed dependency of the OFR on eccentricity, the sum of the outputs of the third layer is weighted, with each unit receiving a weight depending on its location:

$$\text{OFR}=\sum L_{3i} e^{-|x_{3i}|/\tau}, \quad (7)$$

where $x_{3i} = x_{2i}$ is the center of the "receptive field" for the ith unit in the third layer, and τ is a space constant. Finally, a scaling factor (essentially a sensorimotor gain) is computed (linear fit with zero intercept) to best match the responses to single strips.

Overall, the model has four parameters. Of these, τ is used to fit the OFRs to single strips, whereas the other three determine the response to the pairs of strips and thus the interaction index. Our choice of an exponential function for the third layer weights is such that its parameters can be chosen so that the model reproduces reasonably well the single strip data for a wide range of the other three parameters, and so the problem of finding the set of parameters that best fits the data can be formulated as two separate, nested, optimization problems. The other three parameters are then used to fit the responses to strip pairs (and thus the interaction index).

In Figure 10, we plot the interaction index, together with the model fits, for our main experiment. In all cases, the response to single strips (not shown) was captured perfectly (r^2 between 0.944 and 0.996, mean 0.981), so that the quality of the interaction index fits is also representative of that to the responses to strip pairs. This very simple model (cyan lines) obviously cannot reproduce facilitatory effects, but it is nonetheless capable of reproducing reasonably well the data from subjects BMS and EJF, who exhibited only limited facilitation. For subject CQ, it obviously fell considerably short for all SFs.

A simple way to add the potential for a facilitatory effect at large separations/small OFR magnitudes is to have the output of the model (OFR in Equation 7) pass through an expansive output non-linearity. Typically, squaring or half-squaring are used as output non-linearities in neural models. Here, however, we opted for a different function, which is only apparently more complex:

$$\mathrm{OFR}^{\mathrm{NL}}=\cosh(\operatorname{arcsinh}(G\cdot \mathrm{OFR}))-1.0, \tag{8}$$

where cosh() is the hyperbolic cosine function and arcsinh() is the inverse hyperbolic sine function. The output of this non-linearity, which has one parameter (G), is 0.0 when the input is 0.0, increases in an expansive manner for small values of the input, and then increases linearly for larger values of the input. G controls where along the non-linearity the model operates. We indicate this extended model as *variant 1*. In Figure 10, we plot the fits obtained with this model (orange line) in all cases in which it significantly improved the quality of the fit (according to both χ^2 and Akaike's Information Criterion tests). The addition of this parameter obviously improves the fits whenever facilitation is observed (orange lines), resulting in a considerable improvement especially for subject CQ.

A further improvement can be obtained by modifying the divisive normalization mechanism (Equation 5), making it localized:

$$L_{3i}^{L}=\frac{\sqrt{L_{2i}}}{1.0+f\left(\sum_j L_{2j} e^{-\frac{|x_{2j}-x_{2i}|}{\tau_n}}\right)}. \tag{9}$$

Here τ_n is a parameter that determines how the outputs of the second layer should be weighted within the normalization pool for each element in the third layer. The weighting function is exponential, so that nearby stimuli interact more strongly than far apart stimuli. The effect of this additional parameter are however very limited. In only two cases (green lines), this model (which we label *variant 2*), with its additional parameter, led to a significant improvement in the fit quality (assessed as before) compared to the variant 1 model (note that the expansive non-linearity introduced in variant 1 was also part of variant 2). In Table 1, we list the parameter values for the fits, providing the parameters for the best fitting model. We also list the value of the denominator in Equation 5 (global normalization, GN), for single strips and pairs.

Discussion

The experiments presented here allow us to draw a few conclusions about the effect of the spatial properties of a motion stimulus on the response generated by the ocular following system. First, we have confirmed that small stimuli can be quite effective at driving ocular following. Even the smallest stimulus used, covering just over 4 deg^2, induced a measurable OFR. Second, we have shown that the location of a (relatively) small stimulus has a large impact on the magnitude (and to a smaller extent on the latency) of the response. Third,

when pairs of stimuli are presented, the OFR elicited is non-linearly related to the responses induced by the individual stimuli: Nearby stimuli result in suppressed responses (relative to a linear summation), and the suppressive effects fade away as the separation between stimuli is increased. Fourth, the interplay between these interactions and the dependency of the responses to single strips on eccentricity leads to an unexpected behavior for the strip pairs: The peak response is not observed for nearby strips but rather for a specific separation that is a function of SF.

Why are OFRs sensitive to stimulus parameters?

As we noted in the Introduction section, there is already compelling evidence to indicate that the ocular following system does not always behave as would be expected of a tracking system. When tested with sinusoidal gratings, the OFR magnitude is tuned to the temporal frequency of the stimulus, not its speed (Gellman et al., 1990; Miles et al., 1986). Similarly, the size of the stimulus affects OFR magnitude and latency (Barthelemy et al., 2006). Our results add to this evidence, showing dramatic effects of spatial arrangement.

Obviously, for a tracking mechanism the ocular following system does not appear to be very good at estimating the speed to be matched. Instead, in the laboratory it often appears to behave in a very primitive way, barely filtering the signals arising from early visual processing stages. To understand why this might occur, it is important to bear in mind that the ocular following system might have evolved to contribute to the stabilization of the image on the retina when a moving observer looks off to one side. To achieve this goal, it needs to track objects in the plane of fixation (Miles, 1998), which in natural conditions presumably contains many patterned stimuli. Since the OFR is generated quickly and in a bottom-up fashion, the cascade of neural operations that determines the OFR might only operate as intended in the presence of extensive and broadband stimuli, whose projections on the retinas move coherently in the same direction. With narrowband, or small and sparse stimuli, the operation might at least partially fail, so that what we measure with these stimuli are neural signals percolating through the system without being properly integrated. To use an analogy from electrical engineering, with typical laboratory stimuli the system might function around an operating point different than the one for which it evolved, rendering it incapable of carrying out its intended function.

One simple way of testing this hypothesis is to verify whether increasing the stimulus area makes the OFRs less sensitive to its spatial arrangement. Sheliga et al. (2008a) measured the responses to one or more (3, 7, or 15) horizontal grating strips 1° high (SF = 0.25 cpd). Indeed, they found that whereas a single central strip was sufficient to induce a strong OFR, adding equally spaced strips only increased the response by 10% (regardless of the number of strips added). Three or more strips thus yielded similar OFRs. To further test this hypothesis, we performed an additional experiment (see Appendix C), in which we used as stimuli either a single horizontal strip at eye level, pairs of strips placed symmetrically above and below eye level, or triplets of strips, composed of one of the pairs plus the central strip. Of course, we already knew from our main experiment what the OFRs looked like for the first two types of stimuli. When we presented the three strips, we found that the OFR variation observed by changing the separation between the two peripheral strips (Figure C1, top row) is much reduced compared to the one we reported for strip pairs (Figure 3). This held for all three subjects and SFs tested (same as in the main experiment). Thus, three strips yielded similar OFRs regardless of their location (within the strict limits of our experimental design).

While the evidence is admittedly still quite limited, we thus propose that what causes the OFRs to be sensitive to stimulus parameters is the suboptimal activation of a neural mechanism that normally pools and integrates information across space, spatial frequency,

and possibly non-Fourier motion signals. Importantly, it is this “integration failure” that makes it possible, by devising appropriate stimuli, to use the OFR as a probe of the visual system. If the ocular following system were to always match stimulus speed, it could not tell us anything about the visual system.

Previous ocular following studies

Ours is not the first study to show that robust OFRs can be evoked with relatively small stimuli. In carrying out our experiments, we actually took a step back from earlier studies, as we investigated even more basic spatial properties of the ocular following system. We will now briefly summarize, and to a certain extent reinterpret in light of our results, some findings from earlier studies.

Sheliga et al. (2008b) added a new dimension, spatial separation, to their previous investigation regarding the interaction between two gratings having different SFs (Sheliga, Kodaka, FitzGibbon, & Miles, 2006). Using strips containing gratings of different SFs, they discovered a variety of interactions, strongly affected by the spatial separation of the strips. More precisely, when the strips moved in opposite directions they interacted strongly only when they were spatially superimposed, whereas their responses summed almost linearly when they were spatially separated. In contrast, when the strips moved in the same direction they always interacted non-linearly, even though these interactions were stronger when the strips overlapped. To explain this complex pattern of behavior, they invoked two mechanisms: local mutual inhibition (irrespective of motion direction) and global divisive normalization (within a single motion direction). A major difference with our study is that we used the same SF for the two strips, whereas the SFs of their strips were separated by more than one octave, and thus at least partially stimulated different SF channels. In addition, they used a single, 2° high strip, located at eye level, at one SF, and two 1° high strips, located symmetrically above and below eye level, at the other SF. According to our findings, both the single strip and the two strips by themselves are subject to complex non-linear interactions. The interactions across SFs on which they focused were thus presumably in addition to interactions within an SF channel; whether and how these two non-linear phenomena interacted with each other is difficult to discern. Despite these differences, our sets of results are quite compatible. First, they also found that when only two strips (of the same SF) are used, increasing the gap between them led to an increased response (their Figures 2A, 3A, and 5B). They only used relatively small separations, up to 10°, and hence could not see the decrease that we saw for even larger separations. When three strips were used, they found a strong sublinear summation (i.e., suppression), which got only moderately weaker with increased strip separation. When we used strip triplets, all of the same SF, we similarly found that the suppression was always strong, even at large separations (Figure C1, bottom row, compare with Figure 5, top row). This behavior is compatible with a global normalization mechanism, as suggested by Sheliga et al. (2008b), which appears to be direction, but not spatial frequency, selective.

Barthelemy et al. (2006) studied how the OFR varies as a function of the diameter of a disk containing a sinusoidal drifting grating. They noted that the response increases steadily as the diameter is increased up to approximately 20° but saturates for larger diameters. In light of these results, they suggested that the OFR might be modeled in terms of a behavioral receptive field, composed of an excitatory center and an inhibitory surround. They further proposed that, in integrating motion signals across the visual field, the ocular following system weights central stimuli more heavily than peripheral ones. An alternative interpretation, which would be in line with our findings, is that the gradient in motion energy efficacy is not caused by differential weighting but rather by the distribution of receptive fields across the retinal space. These two hypotheses make different predictions in terms of the effect of SF: If the distribution of receptive fields matter, the relationship between

stimulus diameter and OFR should vary as function of SF. If instead the center were behaviorally more important than the periphery, there would be no reason for SF to affect that relationship.

Like others before us (Barthelemy, Perrinet, Castet, & Masson, 2008; Masson & Castet, 2002; Sheliga et al., 2005), we found that the OFR saturates for rather low contrasts, indicating that a contrast normalization mechanism is at work. Using a stimulus contained within a 20° disk, Barthelemy et al. (2008) and Masson and Castet (2002) fit a Naka–Rushton function to their contrast response curve and found a value for its semi-saturation parameter very similar to that reported here with much smaller stimuli (around 10%). However, with a full-field stimulus Sheliga et al. (2005) found a much lower semi-saturation contrast (3.9% when the SF of the stimulus was 0.153 cpd and 5.7% for SF = 0.458 cpd). These values are considerably smaller than those found with our thin strips (11.0% in BMS and 12.4% in CQ). Since the experimental conditions and analysis methods were very similar in the two studies, and subject BMS actually participated in both, it is likely that the stimulus is the determining factor for this difference. One possible explanation is that, in determining the OFR, the stimulus energy is summed across space, so that as the stimulus area increases the contrast needed to reach saturation (or semi-saturation) decreases. This explanation would be compatible with the observation that for neurons in monkey MT the semi-saturation contrast decreases as the size of a stimulus centered on their receptive field increases, up to the classical RF size (Sclar, Maunsell, & Lennie, 1990). There are however reasons to be skeptical. First of all, Masson et al. used stimuli much larger than ours but found a semi-saturation contrast very similar to ours. Second, Sheliga et al. (2008a) found that the contrast response curve did not change much as they presented 1, 3, 7, or 15 strips (with coverage increasing from 3.3% to 50%). It was only when they increased coverage to 100% that they found a drastic decrease in semi-saturation contrast (their Figure 2). This was mostly caused by a drastic *decrease* in OFRs when the stimulus covered the entire screen (compared to the 50% coverage condition), more accentuated for high than for low contrast. Thus, it is the full screen condition that appears to be anomalous. Further experiments will be necessary to bring clarity, but it is apparent that the contrast response curve might be an important tool in our efforts to understand the process underlying stimulus integration.

In addition to these studies in human subjects, studies in monkeys have reported similar results. Masson and Perrinet (2012) have repeated their experiment in monkeys and found very similar results. Benson and Guo (1998) also found that response increases with the diameter of a disk stimulus. In addition, they changed the location of a 10° diameter stimulus and found that the response decreases with eccentricity (only a single high SF grating was used, though). Niu and Lisberger (2011) used small patches of drifting random dots and found results comparable to those of Sheliga et al. (2008b), with the effects depending on whether the patches were superimposed or separated. These studies indicate that monkeys and humans behave very similarly, as had been already reported in the past for many other properties of the OFR (Masson & Perrinet, 2012; Miles, 1998; Miles & Sheliga, 2010). This bodes well for our prospects of pinpointing the neural processes that underlie this behavior.

A framework to interpret our findings

In the remainder of this paper, we will place our results in the broader context of what has been learned about the spatial properties of the visual system from other types of experiments. In addition, we will speculate on what our experiments contribute to that body of evidence.

To speculate on the neural mechanisms that might give rise to our findings, we must first make some educated guesses about how OFRs are generated. A general review of the neural pathways that underlie ocular following movements is beyond the scope of this study and can be found elsewhere (Masson & Perrinet, 2012). Here we will just note that it has been established that the cortical output of the ocular following drive resides in areas MT and MST. These signals are then channeled through the pontine nuclei and the cerebellum to reach the motoneurons innervating the extraocular muscles.

We assume that the spatial properties investigated here are of cortical origin and are not mediated, or substantially altered, by subcortical processing. We further assume that the readout of MT/MST activity is rather simple, e.g., a weighted sum. Such a simple readout mechanism has been shown to account remarkably well for the properties of another short-latency visual tracking mechanism, the disparity vergence response (Takemura, Inoue, Kawano, Quaia, & Miles, 2001).

Unfortunately, very little is currently known about how the activity of MT/MST neurons depends on the spatial properties of the stimulus. Recanzone, Wurtz, and Schwarz (1997) recorded from MT and MST neurons in awake behaving monkeys while presenting two small object stimuli in the neuron's receptive field. The stimuli always moved in different directions, following trajectories that intersected in the center of the receptive field. They found that the response to the pair was reasonably well predicted by the average of the responses to the two stimuli individually. There was thus a considerably sub-linear interaction, in both areas.

Britten and Heuer (1999) studied instead the responses to pairs of identical small Gabor patches moving briefly within the receptive field of MT cells. The stimuli had a spatial frequency and orientation that were optimal for the neuron and moved in the same direction (the preferred direction for the neuron). These authors also found that the response to the pair was smaller than the sum of the responses to the two individual stimuli. However, they noted that the response to the pair tended to be skewed toward the response of the most effective stimulus (i.e., the one closer to the center of the receptive field).

It is not immediately clear how the single-unit phenomena described above would, at a population level, give rise to the behavior we observed. Obviously, the stimuli used in these experiments are quite different than those we used. Nonetheless, the type of neuronal behavior described is compatible with a spatial normalization mechanism (or possibly a cascade of such mechanisms). As a working hypothesis, we will thus simply assume that a sequence of stages characterized by linear filters, output non-linearities, normalization mechanisms, and increasing receptive field sizes account for the behavior we observe. The simple model that we described earlier is a very basic member of that family of models. We will use it as a framework to illustrate the processes that might underlie our experimental results.

Effect of eccentricity

The relationship between strip location, SF, and OFR that we measured matches the known effect of eccentricity on contrast sensitivity. Contrast sensitivity is defined as the reciprocal of the minimum contrast necessary to detect a grating; it decreases with eccentricity, more quickly for high than for low spatial frequencies (Pointer & Hess, 1989; Robson & Graham, 1981), just as we found for OFRs. Conversely, when the sensitivity is plotted as a function of SF for different eccentricities, the larger the eccentricity, the lower the SF associated with peak sensitivity. The spatial frequency tuning curve is thus skewed toward high frequencies in the center and toward low frequencies in the periphery. This feature can also be readily

observed in our data (Figure 2), even though the number of SFs tested is too small to plot an SF tuning curve.

The simplest explanation for these findings is that they reflect the distribution of receptive fields in early visual areas: Cells responsive to high SFs are denser in the center of the visual field, whereas cells that respond to low SFs are more uniformly distributed (De Valois, Albrecht, & Thorell, 1982; Tootell, Silverman, & De Valois, 1981). A strip at eye level is thus highly effective over a large range of SFs, but as its distance from eye level increases it becomes less and less capable of activating high SF channels. For ease of implementation, in our simple model we embedded this concept by scaling the output of the third layer as a function of eccentricity (Equation 7). Presumably, this scaling occurs much earlier.

Two-strip interactions

Our experiments revealed the presence of powerful nonlinear interactions between two stimuli. The strength of this interaction varied as a function of the separation between the stimuli, leading to strong suppression for nearby stimuli and much weaker suppression or even facilitation for far apart stimuli. This type of phenomenon has been investigated in several perceptual studies, obviously with a quite different paradigm. Typically, the subject needs to estimate the contrast of a central stimulus (a circular disk containing a sinusoidal grating), with or without flankers (usually either other grating disks or a grating annulus). When the flanking stimulus is an annulus contiguous with the center, generally the center stimulus is suppressed (i.e., its contrast appears lower in the presence of the annulus; Cannon & Fullenkamp, 1993; Xing & Heeger, 2000, 2001). The strength of the interactions usually increases with the size of the flanker but only up to a point (Cannon & Fullenkamp, 1991, 1993). These results are compatible with our finding for abutting strips: Suppression is observed in all conditions tested. When small flanking patches are arranged around a central disk, or when a non-contiguous grating annulus is used, suppression is similarly found (Cannon & Fullenkamp, 1991, 1996). However, the farther the flankers, the weaker the suppression. As the separation between the two increases, eventually facilitation takes over, in some subjects more than in others (Nurminen, Peromaa, & Laurinen, 2010). This is exactly what we found.

One aspect of our results for which we are unable to find a parallel in the psychophysics literature is the observation that the peak response to two strips is obtained when they are presented at a given separation, not when they are abutted at eye level. Given the OFR/perception similarities noted above regarding responses to a single stimulus and suppressive interactions, it is tempting to speculate that an appropriate study, measuring either contrast sensitivity or pedestal masking, might unveil a perceptual correlate of this phenomenon.

What neural mechanisms might be responsible for the non-linear interactions between two stimuli? The perceptual findings summarized above have been fit (Cannon & Fullenkamp, 1996; Xing & Heeger, 2001) using models that are based on divisive normalization and that rely on properly weighting both the stimulus and the flanker signals. Our simple model falls in the same class of models and was indeed inspired by them. A close inspection of the data, and of how our model manages to reproduce it, might give us some hints about the origin of the interactions.

The data reveal two clear dependencies on SF: the decay of the response with eccentricity for single strips (Figure 2) and the separation associated with peak response for the pairs (Figure 4). As previously mentioned, in our model τ determines the former. The latter is affected by both τ and σ_e: Other things being equal, the peak shifts toward smaller separations as either parameter is reduced. It is however important to note that the peak arises only because of the suppressive (normalization) mechanism. In particular, it is crucial

to have a strong suppressive interaction between nearby stimuli, which fades away with larger separations. The space constant of this mechanism is thus the main determinant of the location of the peak (other things being equal). In our model, this space-dependent suppressive interaction is mediated by the compressive non-linearity in the third stage, which acts as a tuned, localized, normalization (Rust, Mante, Simoncelli, & Movshon, 2006). We chose, quite arbitrarily, a square root non-linearity: A lower power would cause the peak to shift toward larger separations, and a higher power would shift it toward zero. We describe this mechanism as localized because its range is limited by the size of the "receptive field" of the second layer units, which is controlled by σ_e (hence the impact of this parameter on the peak location).

A normalization mechanism that provides maximal suppression for nearby stimuli, and no suppression for far apart stimuli, is sufficient to capture the peak separation for strip pairs. However, it always asymptotes to a null suppression, which is different from what we observed. To remedy this, we used a second normalization mechanism (denominator of Equation 5), in which the activity of all units in the third layer is divided by a function (Equation 6) of the summed activity across all the units in the second layer. This is a classic global divisive normalization. This two-step scheme is not unique, and we only chose it because it captures our basic findings with a small number of free parameters. Any scheme in which nearby stimuli interact strongly, but even far apart ones can affect each other, could work (e.g., the one proposed by Cannon & Fullenkamp, 1996).

The type of normalization described above is not sufficient to account for all of our findings. More precisely, it cannot produce facilitation, which we have observed, and it predicts a clear dependency of I_I on SF, which is not discernible in our data (see cyan lines in Figure 10). However, it must be noted that in our experiments facilitation was clearly observed only in one subject and only when the OFRs were very weak (see Figure B1); the same can be said of the results in perceptual experiments (Nurminen et al., 2010). Thus, while it is certainly possible that some genuine facilitation mechanism is present, a more conservative explanation might be preferable. In fact, we found that a simple output non-linearity (Equation 8) is sufficient to account for most of the facilitation we observed (orange lines in Figure 10). As an added bonus, this static non-linearity also breaks the dependency of I_I on SF, reconciling the normalization model with the data.

Effect of contrast

Most of our experiments were carried out using stimuli of an intermediate contrast (32%). However, in some experiments we also varied the contrast to quantify its impact. We found that: (1) a contrast normalization mechanism is at work, since the OFR to single strips saturates for rather low contrasts; (2) this mechanism operates in the same manner across space; and (3) large variations in contrast have only a moderate impact on the interaction index.

Our second finding indicates that the contrast response curve is remarkably consistent across space, making the effects of location and contrast (for a given stimulus size) separable. We are not aware of physiological studies that have explicitly investigated this issue in primates.

We were surprised by our third finding. Since many studies (Cavanaugh et al., 2002; Kapadia et al., 1999; Kohn & Smith, 2005; Levitt & Lund, 1997; Nauhaus et al., 2009; Polat et al., 1998; Sceniak et al., 1999) had revealed that the spatiotemporal properties of receptive fields in primary visual cortex are affected by contrast and, in particular, that surround suppression gives way to spatial summation as contrast decreases, we expected considerably weaker suppression at low contrast. While we found a significant change in this direction, the magnitude of this effect was rather small, much smaller than that observed in single

units. Furthermore, with OFRs large changes were only observed at very low contrast (less than 6%; see Figure 8). In contrast, in single-unit studies changes were readily observed throughout the contrast range (e.g., lowering contrast from 70% to 50%, or from 30% to 15%, induced large changes in most cells). It must however be kept in mind that these studies were conducted in primary visual cortex, where the strength of the contrast normalization mechanism is on average relatively weak (median c_{50} = 33%; Sclar et al., 1990). It is possible that this large effect of contrast reflects mostly the behavior of neurons in the parvocellular pathway and that would be much less prominent in a later area, such as MT, where neurons are characterized by stronger contrast normalization (median c_{50} = 7% with large stimuli, lower with smaller stimuli), or in V1 neurons belonging to the magnocellular pathway.

The small vertical shift in the I_I curve observed as contrast is reduced (Figure 7) can be reproduced by weakening the normalization mechanism. In our simple model, weakening the strength of the input is actually sufficient to shift I_I upward (in part by decreasing the effect of the global divisive normalization and in part by increasing the effect of the output non-linearity). This reliance on a weaker input strength to explain changes in I_I is however problematic. First of all, in our model changes in signal strength much larger than those observed in the contrast data are needed to cause the required changes in I_I. More importantly, when we modulated the temporal frequency of our stimuli (Figure B3) we found that large magnitude changes barely affected the interaction index. We thus tend to favor the hypothesis that a contrast-dependent reduction in the gain of the normalization mechanism is necessary. A similar weakening by contrast of a divisive normalization center–surround mechanism has been shown to account for the changes observed at the single neuron level (Cavanaugh et al., 2002).

Effect of strip width

Changing the width of our strips had a dramatic effect on the OFR we measured. Both the magnitude of the responses and the interaction index were affected. It is important to note that the change in response magnitude was in a sense more “genuine” than the change caused by contrast changes. Decreasing contrast from 64% to 8% resulted in a conspicuous change in response latency (13–14 ms), which accounted for a large fraction of the change in our stimulus-based measurements: The responses were greatly delayed and slightly (8% on average) attenuated. On the contrary, reducing the width of the strip from 32° to 8° had only very small effects on response latency (3–4 ms): The responses were greatly attenuated (Figure 9) and slightly delayed. This is very similar to what we observed when we modulated the temporal frequency of the stimulus: The magnitude of the responses was greatly reduced (Figure B3), but if anything their latency was slightly shorter. The impact of temporal frequency and strip width on the interaction index was however vastly different. To make this point clearly, we can start by considering the data from subject BMS. With strips at 4° of elevation, doubling the TF of a screen-wide strip lowered the OFR to the strip from 0.85°/s to 0.35°/s (Figure B3, top left panel). I_I was however completely unaffected by TF (bottom left panel). When the width of the strips, at the same elevation, was reduced from 32° to 16°, the OFR to the strip also dropped, but not by as much, going from 0.61°/s to 0.45°/s (Figure 9, top left panel). Yet a sizeable increase in I_I was observed (top right panel). Similar comparisons can be drawn for the other data points and subjects.

Since this comparison rules out an output non-linearity as being responsible for the difference, our working hypothesis is that the changes in the interaction index associated with changes in strip width are mostly a reflection of changes in normalization strength. An output non-linearity might then further enlarge this difference. Under this scenario, changes in the strength of normalization should thus be different when the same set of neurons is activated less strongly (as when we doubled TF) than when fewer neurons are activated (as

when we reduced strip width). One highly speculative possibility is that there are actually two normalization mechanisms, one that operates for collinear stimuli and the other for side-by-side stimuli. Reducing the width of our strips might have a large impact on the former, making the system more sensitive to changes in the input to the latter. Further experiments will obviously be necessary to investigate this possibility.

Future directions

Our investigation shows that using one or more small stimuli to induce OFRs provides new opportunities to probe the visual system. At the same time, it would be foolish to deny the largely speculative nature of our efforts to explain our observations in neurophysiological terms. Obviously, we still know too little about the visual system to explain how the cooperation of a large number of neurons across a large number of brain areas gives rise to the responses we measure. The model we presented is rudimentary, and additional experiments will be required to improve on it.

Besides the complexity of the system, an additional hindrance is represented by the fact that our experimental conditions are quite different from those in which neurophysiological experiments are usually carried out. In most such studies, the stimulus is optimized, and thus different, for each cell. It is then quite difficult to infer from the responses of many cells to many different stimuli the population response to a single stimulus. Fortunately, as multi-unit recordings become more widespread, this problem will be ameliorated, and it will become possible to directly compare cortical activity and OFRs, an approach that has been very successful for short-latency disparity vergence responses (Takemura et al., 2001). Conversely, our findings indicate that the stimuli commonly used in neurophysiological experiments studying motion processing in MT and MST are most likely sufficient to induce OFRs. A systematic measurement and analysis of OFRs in the context of those experiments will considerably accelerate our understanding of the neural basis of the ocular following system. In turn, this will enable behavioral experiments such as ours to become precise and powerful probes of the human visual system, in both physiologic and pathologic states.

Acknowledgments

This research was supported by the Intramural Research Program of the National Eye Institute, NIH. We thank Bruce Cumming, Richard Krauzlis, and three anonymous reviewers for their constructive comments.

References

Anderson S, Burr D. Spatial summation properties of directionally selective mechanisms in human vision. Journal of the Optical Society of America A. 1991; 8:1330–1339.

Banks M, Sekuler A, Anderson S. Peripheral spatial vision: Limits imposed by optics, photoreceptors, and receptor pooling. Journal of the Optical Society of America A. 1991; 8:1775–1787.

Barthelemy F, Fleuriet J, Masson G. Temporal dynamics of 2D motion integration for ocular following in macaque monkeys. Journal of Neurophysiology. 2010; 103:1275–1282. [PubMed: 20032230]

Barthelemy F, Perrinet L, Castet E, Masson G. Dynamics of distributed 1D and 2D motion representations for short-latency ocular following. Vision Research. 2008; 48:501–522. [PubMed: 18221979]

Barthelemy F, Vanzetta I, Masson G. Behavioral receptive field for ocular following in humans: Dynamics of spatial summation and center–surround interactions. Journal of Neurophysiology. 2006; 95:3712–3726. [PubMed: 16554515]

Benson P, Guo K. Short-latency ocular following of motion by monkeys during a fixation task. Neuroreport. 1998; 9:3981–3987. [PubMed: 9875740]

Bracewell, R. Fourier analysis and imaging. New York: Kluwer Academic/Plenum; 2003.

Brainard D. The psychophysics toolbox. Spatial Vision. 1997; 10:433–436. [PubMed: 9176952]

Britten K, Heuer H. Spatial summation in the receptive fields of MT neurons. Journal of Neuroscience. 1999; 19:5074–5084. [PubMed: 10366640]

Busettini C, Fitzgibbon E, Miles F. Short-latency disparity vergence in humans. Journal of Neurophysiology. 2001; 85:1129–1152. [PubMed: 11247983]

Cannon M, Fullenkamp S. Spatial interactions in apparent contrast: Inhibitory effects among grating patterns of different spatial frequencies, spatial positions and orientations. Vision Research. 1991; 31:1985–1998. [PubMed: 1771782]

Cannon M, Fullenkamp S. Spatial interactions in apparent contrast: Individual differences in enhancement and suppression effects. Vision Research. 1993; 33:1685–1695. [PubMed: 8236856]

Cannon M, Fullenkamp S. A model for inhibitory lateral interaction effects in perceived contrast. Vision Research. 1996; 36:1115–1125. [PubMed: 8762716]

Cavanaugh J, Bair W, Movshon J. Nature and interaction of signals from the receptive field center and surround in macaque v1 neurons. Journal of Neurophysiology. 2002; 88:2530–2546. [PubMed: 12424292]

Collewijn H, van der Mark F, Jansen T. Precise recording of human eye movements. Vision Research. 1975; 15:447–450. [PubMed: 1136166]

Daugman J. Two-dimensional spectral analysis of cortical receptive field profiles. Vision Research. 1980; 20:847–856. [PubMed: 7467139]

Daugman J. Spatial visual channels in the Fourier plane. Vision Research. 1984; 24:891–910. [PubMed: 6506478]

Daugman J. Uncertainty relation for resolution in space, spatial frequency, and orientation optimized by two-dimensional visual cortical filters. Journal of the Optical Society of America A. 1985; 2:1160–1169.

De Valois R, Albrecht D, Thorell L. Spatial frequency selectivity of cells in macaque visual cortex. Vision Research. 1982; 22:545–559. [PubMed: 7112954]

De Valois, R.; De Valois, K. Spatial vision. Oxford, UK: Oxford University Press; 1988.

Efron, B. The jackknife, the bootstrap, and other resampling plans. Philadelphia: SIAM; 1982.

Foley J, Varadharajan S, Koh C, Farias M. Detection of Gabor patterns of different sizes, shapes, phases and eccentricities. Vision Research. 2007; 47:85–107. [PubMed: 17078992]

Gellman R, Carl J, Miles F. Short latency ocular-following responses in man. Visual Neuroscience. 1990; 5:107–122. [PubMed: 2278939]

Grossberg S. Contour enhancement, short term memory, and constancies in reverberating neural networks. Studies on Applied Mathematics. 1973; 52:213–257.

Hays, A.; Richmond, B.; Optican, L. A UNIX-based multiple process system for real-time data acquisition and control. WESCON Conference Proceedings; 1982. p. 1-10.

Heeger D. Normalization of cell responses in cat striate cortex. Visual Neuroscience. 1992; 9:181–197. [PubMed: 1504027]

Kapadia M, Westheimer G, Gilbert C. Dynamics of spatial summation in primary visual cortex of alert monkeys. Proceedings of the National Academy of Sciences of the United States of America. 1999; 96:12073–12078. [PubMed: 10518578]

Kohn A, Smith M. Stimulus dependence of neuronal correlation in primary visual cortex of the macaque. Journal of Neuroscience. 2005; 25:3661–3673. [PubMed: 15814797]

Levitt J, Lund J. Contrast dependence of contextual effects in primate visual cortex. Nature. 1997; 387:73–76. [PubMed: 9139823]

Masson G. From 1D to 2D via 3D: Dynamics of surface motion segmentation for ocular tracking in primates. The Journal of Physiology. 2004; 98:35–52.

Masson G, Castet E. Parallel motion processing for the initiation of short-latency ocular following in humans. Journal of Neuroscience. 2002; 22:5149–5163. [PubMed: 12077210]

Masson G, Perrinet L. The behavioral receptive field underlying motion integration for primate tracking eye movements. Neuroscience and Biobehavioral Reviews. 2012; 36:1–25. [PubMed: 21421006]

Masson G, Rybarczyk Y, Castet E, Mestre D. Temporal dynamics of motion integration for the initiation of tracking eye movements at ultra-short latencies. Visual Neuroscience. 2000; 17:753–767. [PubMed: 11153655]

Masson G, Yang D, Miles F. Reversed short-latency ocular following. Vision Research. 2002a; 42:2081–2087. [PubMed: 12169427]

Masson G, Yang D, Miles F. Version and vergence eye movements in humans: Open-loop dynamics determined by monocular rather than binocular image speed. Vision Research. 2002b; 42:2853–2867. [PubMed: 12450510]

Michelson, A. Studies in optics. Chicago: University of Chicago Press; 1927.

Miles F. The neural processing of 3-D visual information: Evidence from eye movements. European Journal of Neuroscience. 1998; 10:811–822. [PubMed: 9753150]

Miles F, Kawano K, Optican L. Short-latency ocular following responses of monkey: I. Dependence on temporospatial properties of visual input. Journal of Neurophysiology. 1986; 56:1321–1354. [PubMed: 3794772]

Miles, F.; Sheliga, B. Motion detection for reflexive tracking. In: Ilg, U.; Masson, G., editors. Dynamics of visual motion processing: Neuronal, behavioral, and computational approaches. New York, NY: Springer; 2010. p. 141-160.

Moulden B, Kingdom F, Gatley L. The standard deviation of luminance as a metric for contrast in random-dot images. Perception. 1990; 19:79–101. [PubMed: 2336338]

Nauhaus I, Busse L, Carandini M, Ringach D. Stimulus contrast modulates functional connectivity in visual cortex. Nature Neuroscience. 2009; 12:70–76.

Niu Y, Lisberger S. Sensory versus motor loci for integration of multiple motion signals in smooth pursuit eye movements and human motion perception. Journal of Neurophysiology. 2011; 106:741–753. [PubMed: 21593392]

Nurminen L, Peromaa T, Laurinen P. Surround suppression and facilitation in the fovea: Very long-range spatial interactions in contrast perception. Journal of Vision. 2010; 10(13):9, 1–13. http://www.journalofvision.org/content/10/13/9. [PubMed] [Article]. 10.1167/10.13.9 [PubMed: 21071576]

Pelli D. The Videotoolbox software for visual psychophysics: Transforming numbers into movies. Spatial Vision. 1997; 10:437–442. [PubMed: 9176953]

Pointer J, Hess R. The contrast sensitivity gradient across the human visual field: With emphasis on the low spatial frequency range. Vision Research. 1989; 29:1133–1151. [PubMed: 2617861]

Polat U, Mizobe K, Pettet M, Kasamatsu T, Norcia A. Collinear stimuli regulate visual responses depending on cell's contrast threshold. Nature. 1998; 391:580–584. [PubMed: 9468134]

Pollen D, Ronner S. Visual cortical neurons as localized spatial frequency filters. IEEE Transactions on Systems, Man, and Cybernetics. 1983; 13:907–916.

Recanzone G, Wurtz R, Schwarz U. Responses of MT and MST neurons to one and two moving objects in the receptive field. Journal of Neurophysiology. 1997; 78:2904–2915. [PubMed: 9405511]

Robinson D. A method of measuring eye movement using a scleral search coil in a magnetic field. IEEE Transactions on Biomedical Engineering. 1963; 10:137–145. [PubMed: 14121113]

Robson J, Graham N. Probability summation and regional variation in contrast sensitivity across the visual field. Vision Research. 1981; 21:409–418. [PubMed: 7269319]

Rust N, Mante V, Simoncelli E, Movshon J. How MT cells analyze the motion of visual patterns. Nature Neuroscience. 2006; 9:1421–1431.

Savitzky A, Golay M. Smoothing and differentiation of data by simplified least squares procedures. Analytic Chemistry. 1964; 36:1627–1639.

Sceniak M, Ringach D, Hawken M, Shapley R. Contrast's effect on spatial summation by macaque V1 neurons. Nature Neuroscience. 1999; 2:733–739.

Sclar G, Maunsell J, Lennie P. Coding of image contrast in central visual pathways of the macaque monkey. Vision Research. 1990; 30:1–10. [PubMed: 2321355]

Sheliga B, Chen K, Fitzgibbon E, Miles F. Initial ocular following in humans: A response to first-order motion energy. Vision Research. 2005; 45:3307–3321. [PubMed: 15894346]

Sheliga B, FitzGibbon E, Miles F. Human ocular following: Evidence that responses to large-field stimuli are limited by local and global inhibitory influences. Progress in Brain Research. 2008a; 171:237–243. [PubMed: 18718307]

Sheliga B, Fitzgibbon E, Miles F. Spatial summation properties of the human ocular following response (OFR): Evidence for nonlinearities due to local and global inhibitory interactions. Vision Research. 2008b; 48:1758–1776. [PubMed: 18603279]

Sheliga B, Kodaka Y, FitzGibbon E, Miles F. Human ocular following initiated by competing image motions: Evidence for a winner-take-all mechanism. Vision Research. 2006; 46:2041–2060. [PubMed: 16487988]

Simon, J. Resampling: The new statistics. Alexandria, VA: Resampling Stats; 1995. www.resample.com

Takemura A, Inoue Y, Kawano K, Quaia C, Miles F. Single-unit activity in cortical area MST associated with disparity-vergence eye movements: Evidence for population coding. Journal of Neurophysiology. 2001; 85:2245–2266. [PubMed: 11353039]

Tootell R, Silverman M, De Valois R. Spatial frequency columns in primary visual cortex. Science. 1981; 214:813–815. [PubMed: 7292014]

Xing J, Heeger D. Center–surround interactions in foveal and peripheral vision. Vision Research. 2000; 40:3065–3072. [PubMed: 10996610]

Xing J, Heeger D. Measurement and modeling of center–surround suppression and enhancement. Vision Research. 2001; 41:571–583. [PubMed: 11226503]

Appendix A

Default OFR response

The presence of a default response for the OFR (i.e., a motor response that is triggered by stimulus motion or by fixation disengagement but that is not direction selective) has not been systematically investigated, but there are reasons to suspect that it might be present. For example, idiosyncratic directional asymmetries in OFR magnitude have been reported, both in humans and in monkeys (Gellman et al., 1990; Miles et al., 1986). Of course, such an asymmetry would be expected if a default motor response were superimposed on a relatively balanced motion stimulus response. Furthermore, when the (considerably smaller) OFR elicited by a single stimulus step (i.e., a two-frame movie) is measured, it is found that large steps in either direction elicit the same response. This response is generally not null and varies from subject to subject (Masson, Yang, & Miles, 2002a).

Since the presence of a default response could have a major impact on our analysis, we further investigated this aspect of the OFR. As we just mentioned, one approach would be to measure the response to very large single-step motion, as done by Masson et al. (2002a). However, the OFR to such step stimuli is usually much more transient than the response to sustained motion stimuli, and different mechanisms might be engaged. An alternative strategy is to present stimuli that are beyond the range of spatial frequencies (SFs) to which the ocular following is known to respond. Since ocular following responds to motion, for a given temporal frequency (TF), low SFs are the best candidates to generate a default response (a very high SF would lead to a barely moving stimulus). We thus measured the SF tuning curve for the OFR, with the intent of finding out whether at very low frequencies leftward and rightward motion trigger the same response, i.e., the default response. Because with full screen stimuli the tuning curves for leftward and rightward movements were still far apart at the minimum SF that we could reach with our apparatus (0.01 cpd), we used instead a very thin strip, only 3 pixels (0.14°) high, centered at eye level. With this stimulus, the tuning curves for leftward and rightward motion converged in all subjects for SFs at or above 0.034 cpd (Figure A1). For ease of representation, each spatial frequency tuning curve in Figure A1 has been fit with a Gaussian function (using the logarithm of SF as the independent variable). Bars indicating ±1 *SEM* are plotted as well, but they generally fall

within the marker for the mean response. Note that as SF is decreased the OFRs converge smoothly toward a value that is not necessarily zero and that is quite different from subject to subject. At the lowest frequency tested, the difference between the OFR induced by leftward and rightward motion was not significant in any of the subjects (unpaired *t* test, $p > 0.01$); in subject CQ, even the second lowest SF did not induce significantly different OFRs. In spite of this, all subjects could correctly perceive the direction of motion of the pattern, at all SFs, in a two-alternative forced choice test. The most conservative explanation for this behavior is that the overall OFR arises from the superposition of a selective and a non-selective component. This non-selective response is the default OFR; such a default, subject specific, response has also been reported for short-latency disparity vergence responses (Busettini, Fitzgibbon, & Miles, 2001), which share many properties with the OFRs (Miles, 1998). Its presence can also be inferred from careful inspection of some previous OFR studies (e.g., Figure 1 in Masson & Castet, 2002).

Based on this finding, we suggest that reporting the difference between the OFRs induced by stimuli moving in opposite directions might always be helpful when dealing with OFRs. Besides improving the signal-to-noise ratio, doing so cancels the default response, if present.

Appendix B

Control experiments

Strip separation vs. response magnitude

In describing the interaction index, we have assumed as its major determinant the separation between two strips. However, in our experimental design, there is a one-toone relationship between strip separation and eccentricity, as the strips in a pair were placed symmetrically around the center. Since we have shown that the magnitude of the OFR induced by a strip is also related to eccentricity, it then follows that I_I should be well predicted by the magnitude of the OFRs that each strip would induce in isolation (a motor property). In Figure B1, we plot the relationship between the interaction index and the response to an individual strip in the pair, for our three subjects. Quadratic regressions to the data sets, computed using weighted least squares, are also shown. Obviously, the fits are quite good, and this possibility needs to be further investigated.

To address this issue, we thus ran an additional experiment, which allowed us to dissociate the impact of OFR magnitude and strip separation on I_I. In this case, we used six locations for individual strips (±2°, ±13.5°, and ±17.5°). Besides the pairs formed from two strips symmetric about eye level, we also presented the pair formed by the strips at +13.5° and +17.5° and that formed by the strips at −13.5° and −17.5°. With this design, we have three independent pairs separated by the same distance (4°) but centered at different eccentricities and thus associated with different OFR magnitudes. Only one SF (0.25 cpd) was used. In Figure B2, we report the result of this experiment in our three subjects. Not surprisingly, pairs centered at eye level (black) follow the same pattern shown in Figure 5 (top row). However, when small separations at larger eccentricities were used (cyan, orange), I_I was very low and very similar to that found for the same separation around eye level. In general for the small separations, there were no significant differences between I_I in the center and the periphery ($p > 0.05$), with the exception of the lower periphery in subject BMS, where I_I was actually significantly smaller ($p < 0.01$) than in the center. This in spite of the fact that the peripheral pairs are associated with OFRs that are much smaller than those of the same-separation central pair and that are between those of the two far apart pairs. The result was the same when pair-based measures were used to evaluate I_I in this experiment. This shows conclusively that OFR magnitude cannot be the only determinant of the inter-actions that I_I

captures: The separation between strips, and thus presumably the connectivity in retinotopically organized areas, must play a role.

Understanding how big a role the magnitude itself plays is more complicated. From Figure B1, it appears clear that, as SF changes, the same OFR magnitude can be associated with rather different values of the I_I; however, separation is often also different in these cases, and it might be argued that different spatial frequency channels might operate around different set points (since the speed of the stimulus is different). To directly tackle this question, we thus performed an additional experiment, in which we manipulated the OFR magnitude without changing location, spatial frequency, or contrast of the stimulus. In this experiment, we changed the temporal frequency of the stimuli, using two high values: 26.67 Hz and 53.33 Hz (60° or 120° grating phase shift between frames). We selected these values because we know from previous studies using large stimuli (Gellman et al., 1990; Miles et al., 1986) that at 26.67 Hz the OFR is still very robust, whereas at 53.33 Hz it is severely curtailed. However, the neural populations underlying the responses are most likely the same, since there is no evidence for cortical cells tuned to such high temporal frequencies (De Valois & De Valois, 1988). We used four locations for individual strips (±0.3° and ±3.8°) and the two pairs formed by strips symmetric about eye level. The effect of temporal frequency was very large and significant ($p < 0.01$), with the OFR elicited by individual strips dropping by 60–65% (Figure B3, top row). However, the interaction index (Figure B3, bottom row) barely changed and never significantly ($p > 0.05$). Note also that with this manipulation, in spite of large changes in OFR magnitude, latency barely changed: The higher temporal frequency/smaller OFR stimulus was actually associated with slightly (1–3 ms) earlier responses.

From these two control experiments, we can thus conclude the following: When two stimuli are presented simultaneously, the resulting OFR is definitely affected by their spatial arrangement and is only marginally related to the magnitude of the OFR that they induce when presented separately. Any multi-stimulus OFR interaction thus most likely arises from processes taking place in retinotopically organized areas.

Contribution of non-Fourier motion

At the long (i.e., upper and lower) edges of our grating strips, the transition between the grating and the background was abrupt (i.e., there was no smooth contrast transition). Accordingly, non-Fourier (or second-order) motion signals were present. In particular, there were terminators that moved in the same direction and at the same speed as the Fourier (or first-order) motion and a sinusoidal contrast modulation that also moved in the same direction but at twice the speed (because of frequency doubling). When first- and second-order motion signals have different directions (e.g., in the so-called barber-pole stimuli), second-order motion energy has been shown to contribute a late (20 ms from response onset) component to OFRs (Barthelemy, Fleuriet, & Masson, 2010; Barthelemy et al., 2008; Masson, 2004; Masson et al., 2000). The potential contribution of these second-order motion signals under our circumstances (same direction as first-order motion) is difficult to evaluate directly and is beyond the scope of our study. However, here we are especially concerned about the impact that they might have on the interaction index, especially when the most central pair of strips is considered. In that case, the separation is such that the pair actually appears as a single, 1.16° high, strip. Thus, whereas for all other pairs there are four non-Fourier motion generating edges, for the central pair there are only two. It is thus conceivable that I_I for the central pair is so low because less non-Fourier motion is present for that pair. The cleanest way to address this question is to simply remove all non-Fourier motion energy from our stimuli. The simplest way of accomplishing this is by replacing the

sinusoidal gratings with random-dot stimuli. With these stimuli, there is no second-order motion, and there is no late OFR component with barber-pole stimuli (Masson et al., 2000).

We thus ran, on two of our subjects, an additional experiment that was in all aspects like our main experiment but using as stimuli strips composed of drifting random dots instead of sinusoidal gratings. Since most of the variation in I_I occurred over ±10° of elevation, we only used the six centermost pair locations. The random-dot stimuli were presented over a uniform gray background (20.8 cd/m^2) and had a 30% coverage. Half of the dots were darker than the background (9.7 cd/m^2) and half were lighter than the background (31.9 cd/m^2). These luminance values were chosen so that the standard deviation of the luminance was the same for this stimulus and for our original 32% contrast grating (Moulden, Kingdom, & Gatley, 1990). The random-dot stimulus drifted at 5 pixels/frame, corresponding to a speed in the center field of 37°/s. This speed was chosen because it had been previously shown to elicit strong OFRs in most subjects (Masson, Yang, & Miles, 2002b). The dots were squares, three pixels on the side, and their centers were randomly distributed across one of 12 rows of pixels. This guaranteed that, even for the central pair, the motion energy of a strip pair was equal to the sum of the motion energy of the single strips composing the pair.

We found that, in both subjects, the OFRs evoked by these stimuli were very similar to those induced by grating strips. The interaction index was thus also very close to that obtained with gratings. In Figure B4, we plot, for both subjects, the interaction index as a function of separation, obtained with RDS (blue dots). Superimposed on the RDS data, we also plot the fit to the interaction index computed for the sinusoidal grating data (0.25 cpd, Figure 5, top row). The differences were obviously minimal, and there was no significant difference across the two data sets (bootstrap difference test, $p > 0.76$ for both subjects). We thus conclude that second-order motion signals have no impact on the measurements reported here. This means that either they do not contribute to the OFRs under our circumstances (same direction as first-order motion signals) or they induce OFRs that have the same dependency on eccentricity and separation as those induced by first-order motion (and thus simply change the gain of the system).

Appendix C

Response to strip triplets

When comparing responses to single strips (Figure 2) and strip pairs (Figure 3), it appears that responses to pairs vary over a smaller range than responses to single strips. This would be expected if some normalization mechanism were at work. A previous study (Sheliga et al., 2008a), using 1° strips, found that when three or more equally spaced strips were presented the OFRs did not change very much. To verify whether this trend of reduced OFR variability for increased coverage holds also under our conditions, we performed an additional experiment, in which we used as stimuli either a single horizontal strip at eye level, pairs of strips placed symmetrically above and below eye level, or triplets of strips, composed of one of the pairs plus the central strip. The strips were always of the same size as in our main experiment (0.58° high), and for the gratings, we used the same three spatial frequencies used in the main experiment. All three subjects were tested. We found that the OFR variation observed by changing the separation between the two peripheral strips (Figure C1, top row) is indeed reduced compared to the one we reported for strip pairs (Figure 3).

We also computed the interaction index; this time defined as

$$I_1 = \frac{\mathrm{OFR}_{\mathrm{TRIPLET}}}{\mathrm{OFR}_{\mathrm{SINGLE}} + \mathrm{OFR}_{\mathrm{PAIR}}}. \quad \text{(C1)}$$

Its value, as a function of the separation between the strips in the pair, is plotted in Figure C1 (bottom row). Its range is obviously more limited than that for strip pairs (Figure 5, top row), never reaching the high values (or facilitation) observed for strip pairs.

It is important to stress that these results apply to our specific experimental design and do not necessarily extend to an arbitrary arrangement of three strips. In particular, in all our triplet conditions, a strip was always present at eye level, and it might play a strong role in activating the normalization mechanism.

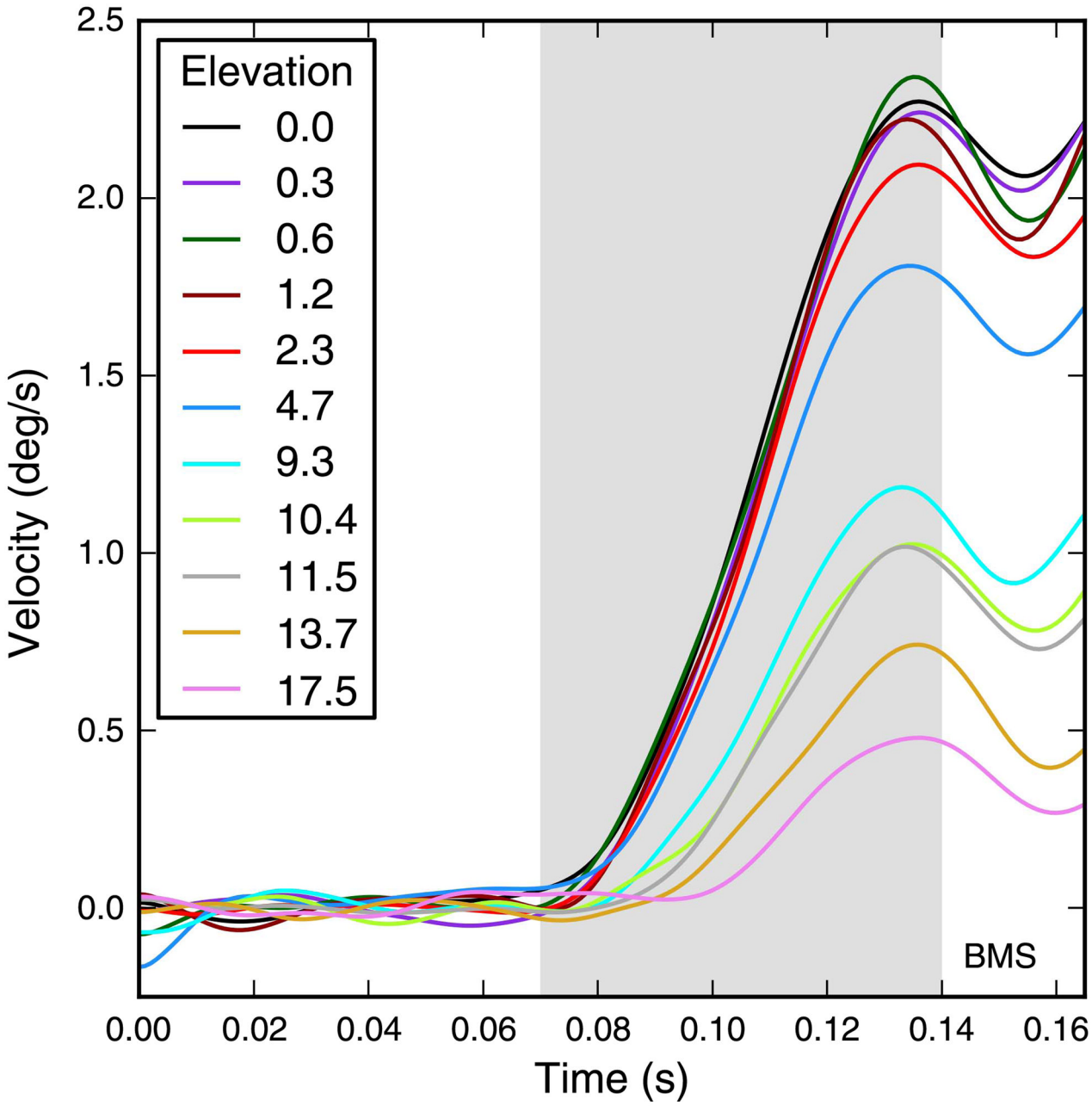

Figure 1.

Quantifying the OFR magnitude. The OFR is a dynamic response. We quantified its magnitude by computing the average eye speed in a time window (shaded region). The duration of the window was such that only the open-loop period of the response was analyzed (i.e., the duration of the window was shorter than the response latency), and it was kept constant (for each subject) across all experiments. Here we plot the difference between the eye velocity induced in subject BMS by single strips moving rightward and leftward. The elevation (i.e., vertical distance of the center of the strip relative to eye level) of each strip is indicated in the legend. Stimulus contrast was 32%. The time window (shaded area) over which the speed was averaged to compute the OFR magnitude in this subject extended from 70 ms to 140 ms relative to the onset of stimulus motion.

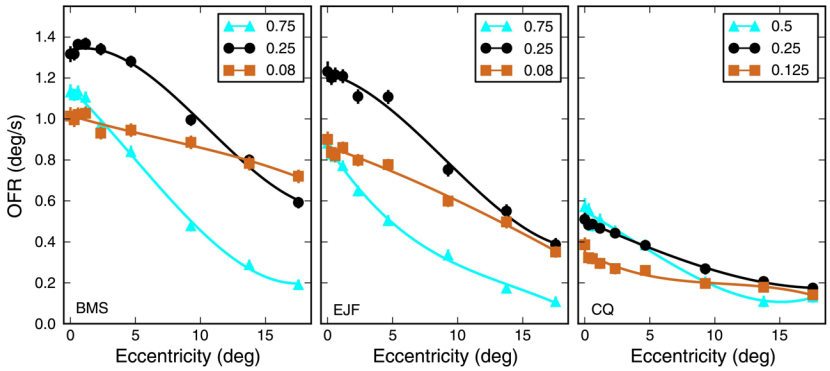

Figure 2.

OFR to individual strips. The response to single strips was affected by both stimulus eccentricity and spatial frequency. In two subjects, the stimuli had SFs of 0.083, 0.25, and 0.75 cpd, whereas in the third subject, 0.125, 0.25, and 0.5 cpd were used. As eccentricity increased, the responses dropped, faster at high than at low SFs. The behavior was consistent across subjects. Mean ± *SEM* is plotted (error bars are often smaller than the marker for the mean and thus barely visible). Cubic fits to the data are plotted.

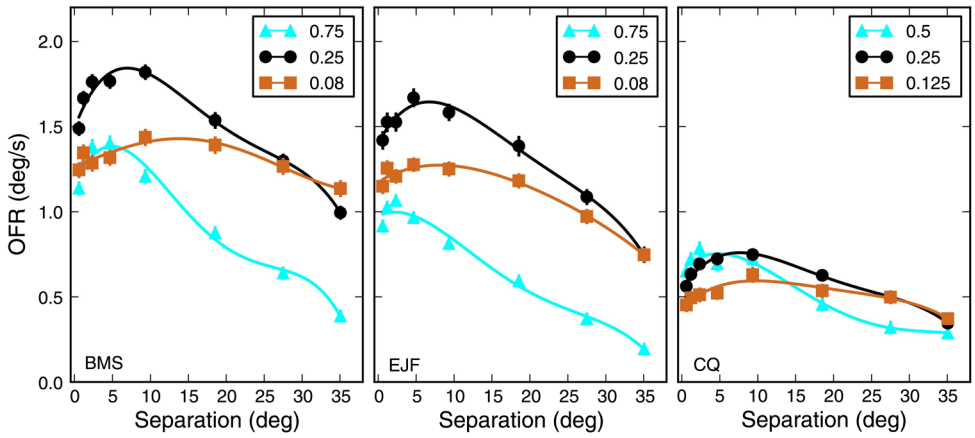

Figure 3.

OFR to strip pairs. The response to a pair of strips was affected by both the separation between strips and spatial frequency. Note that with separation we refer to the distance between the center of the two strips, not to the empty space between them. The separation for the pair composed of the two strips centered at ±0.3° is thus 0.6°, even though in reality the stimulus appears as a single large strip. The most notable difference relative to responses to single strips (Figure 2) is that the peak response occurred when eccentric stimuli were used. The location of the peak varies as a function of SF, with lower SFs peaking at larger separations. Fourth-order polynomial fits are plotted through the data.

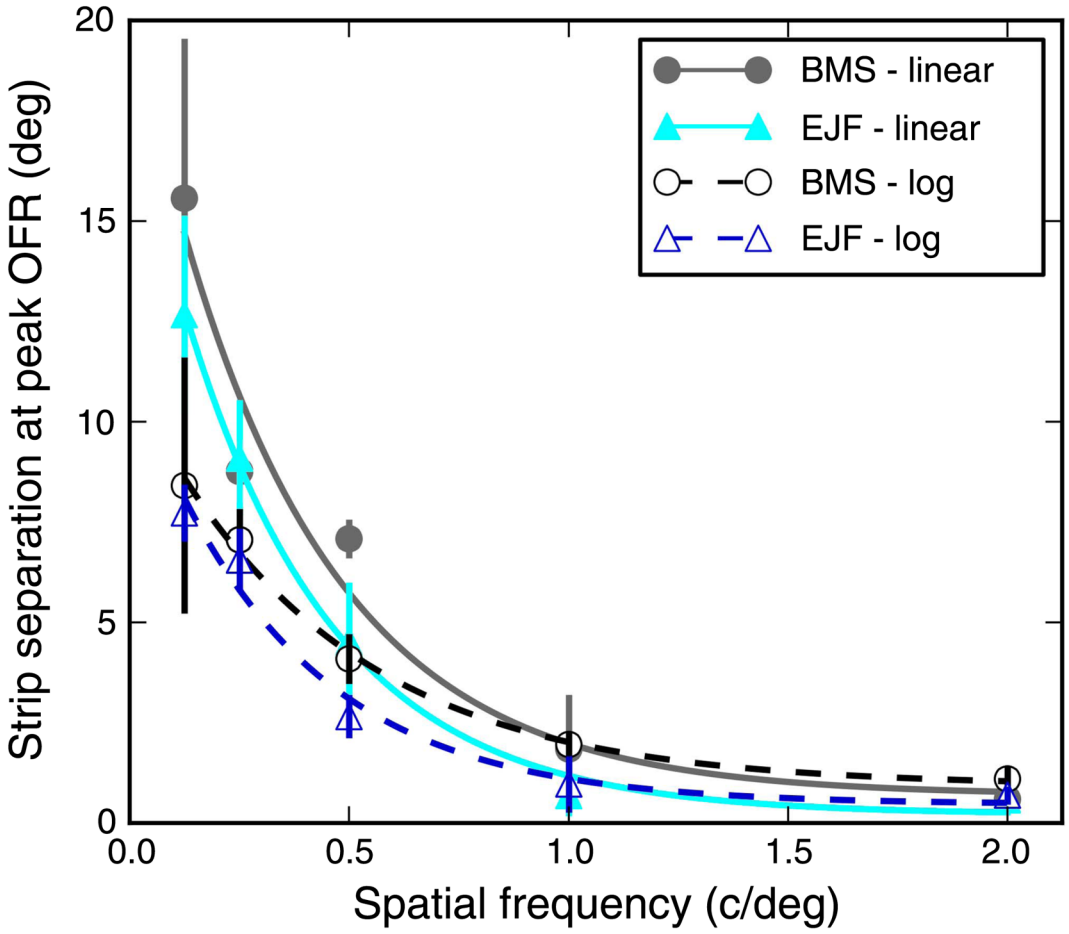

Figure 4.

Strip separation associated with peak OFR. In two subjects, we evaluated the strip separation associated with the peak OFR response, over a range of SFs. The peak separation was inferred from fits to the raw data (see Figure 3), and a bootstrap algorithm was used to compute confidence intervals. The peak separation was affected by the order of the fit used and on whether the fit was performed on a linear or on a logarithmic separation scale. Here the results of third-order fits are shown, for both linear and logarithmic scales. In all cases, there is an inverse relationship between SF and peak separation. Means ± *SEM* are plotted, together with a decaying exponential fit.

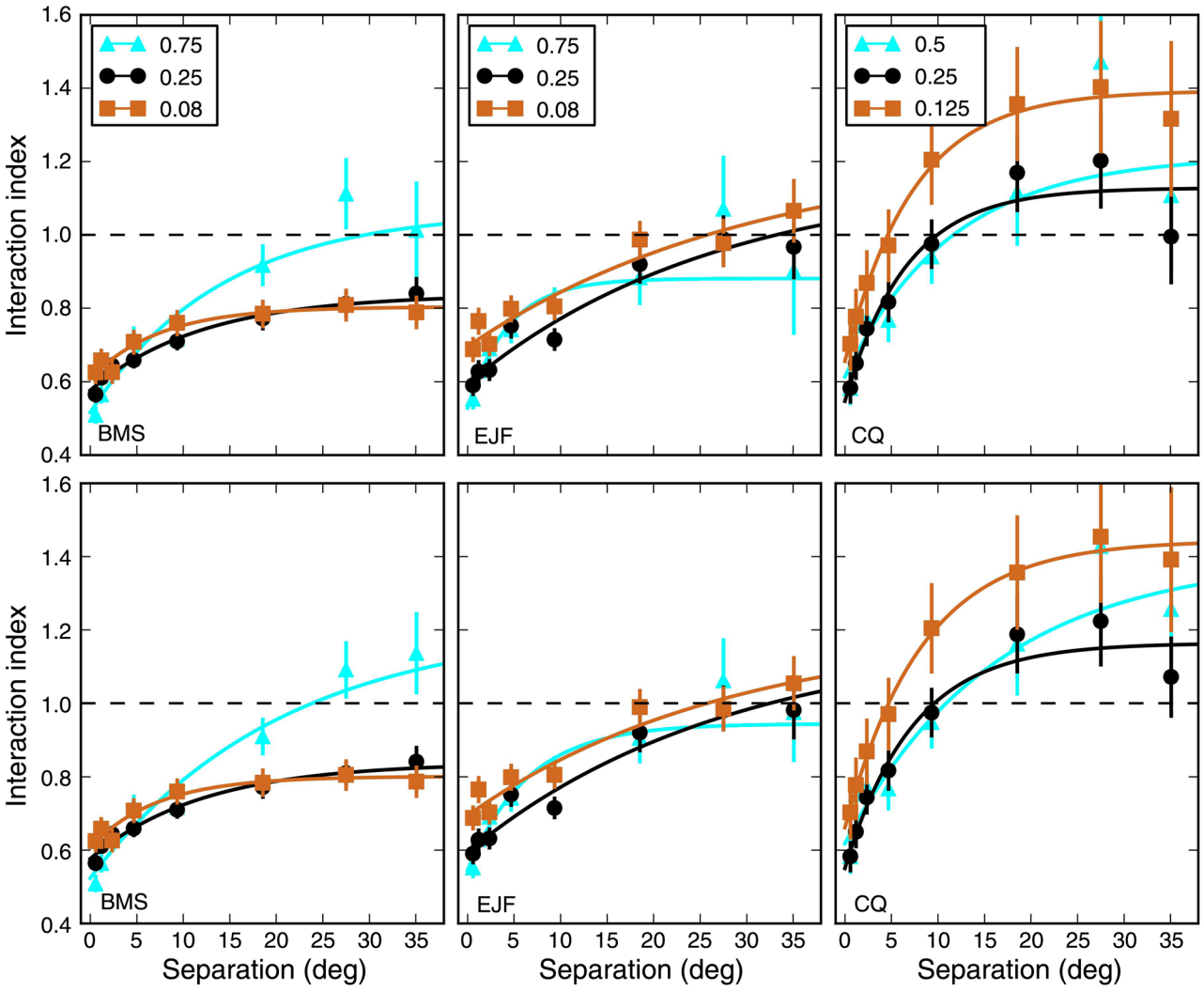

Figure 5.

Interaction index as a function of strip separation and SF. When two strips were presented, the OFR was generally different than either the response to a single strip or the sum of the responses to the individual strips. When the two strips were close together, they interacted in a strong suppressive manner, so that the response to the strips was only somewhat larger than the response to a single strip. However, when the separation increased the response to the pair became relatively stronger. In some conditions, and in some subjects more than in others, at large separation there was facilitation, so that the response to the pair was larger than the sum of the responses to the individual strips. Top row: Interaction index calculated using stimulus-based measures. Bottom row: Interaction index calculated using pair-based measures. This was potentially important for eccentric stimuli, when the latency of the response could be quite different from that for more central stimuli (Figure 1). However, the differences are modest. Note that in a majority of the cases the last point was lower than the next-to-last one. However, this effect was not significant, neither at the level of individual points (bootstrap difference test, $p > 0.24$) nor as a trend (bootstrap group difference test, $p > 0.15$). Error bars indicate $\pm SEM$. Dashed line indicates linear summation. The data were fit using an exponential function with three parameters: $I_I = I_{I0} + G\,(1 - e^{-\mathrm{sep}/\sigma})$.

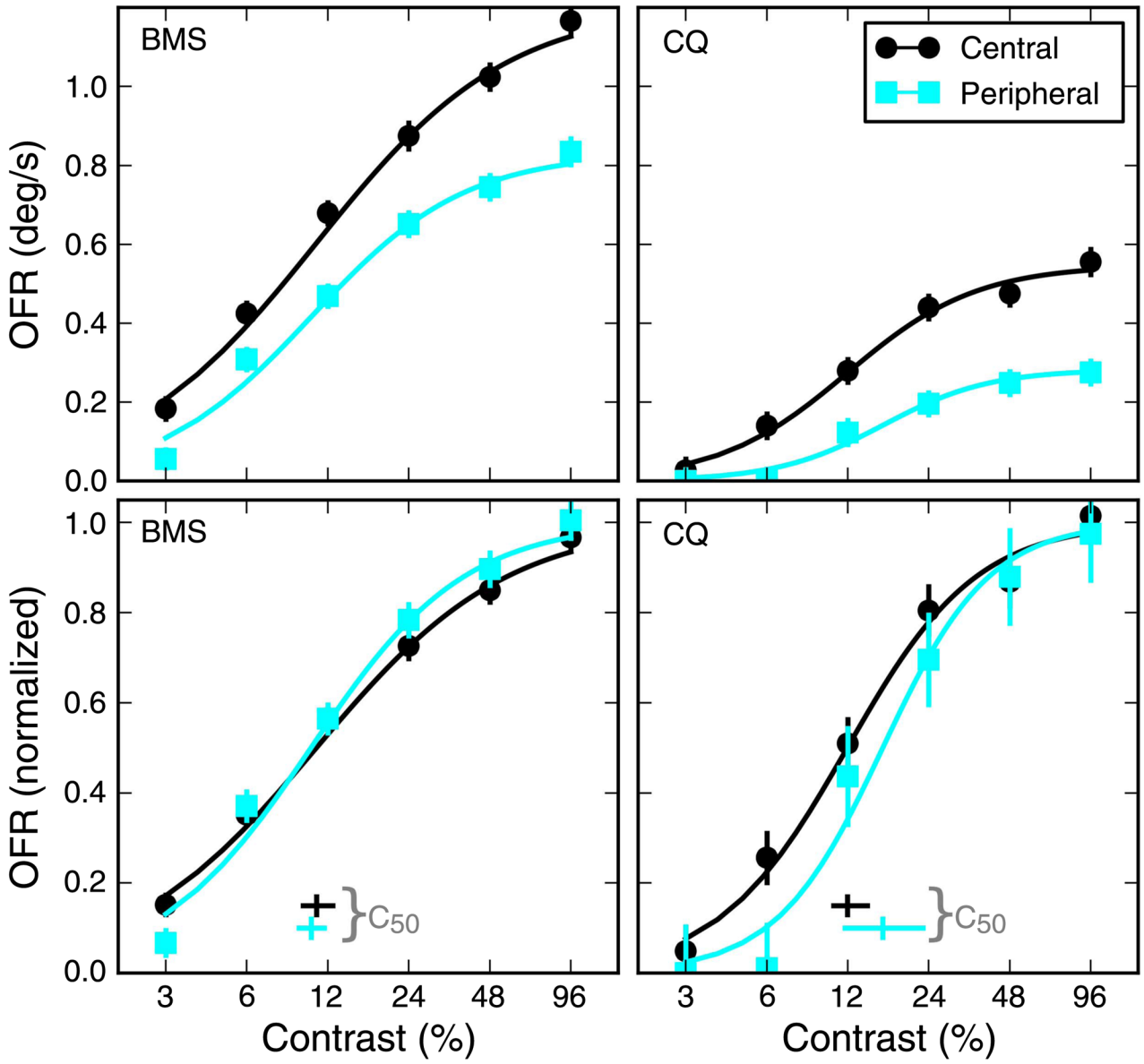

Figure 6.

Contrast response curves. Contrast has a large impact on the behavior of neurons throughout the visual system, affecting both latency and magnitude of the responses. Here we measured the OFR to a small strip presented either centrally or peripherally (±9.3°). We found that in both subjects the response saturated rather quickly, obviously at a higher level for central than for peripheral stimuli (top row). Naka–Rushton fits are shown. When the responses are normalized (bottom row), it also becomes apparent that contrast and eccentricity affect the response mostly independently of each other. Normalization was based on the fits, i.e., each curve from the top panels was divided by its respective R_{max}. Means ± *SEM* are plotted, but the error bars are usually smaller than the marker for the mean. In the bottom row, median value and 68% confidence interval for the semi-saturation parameter (c_{50}) are also shown.

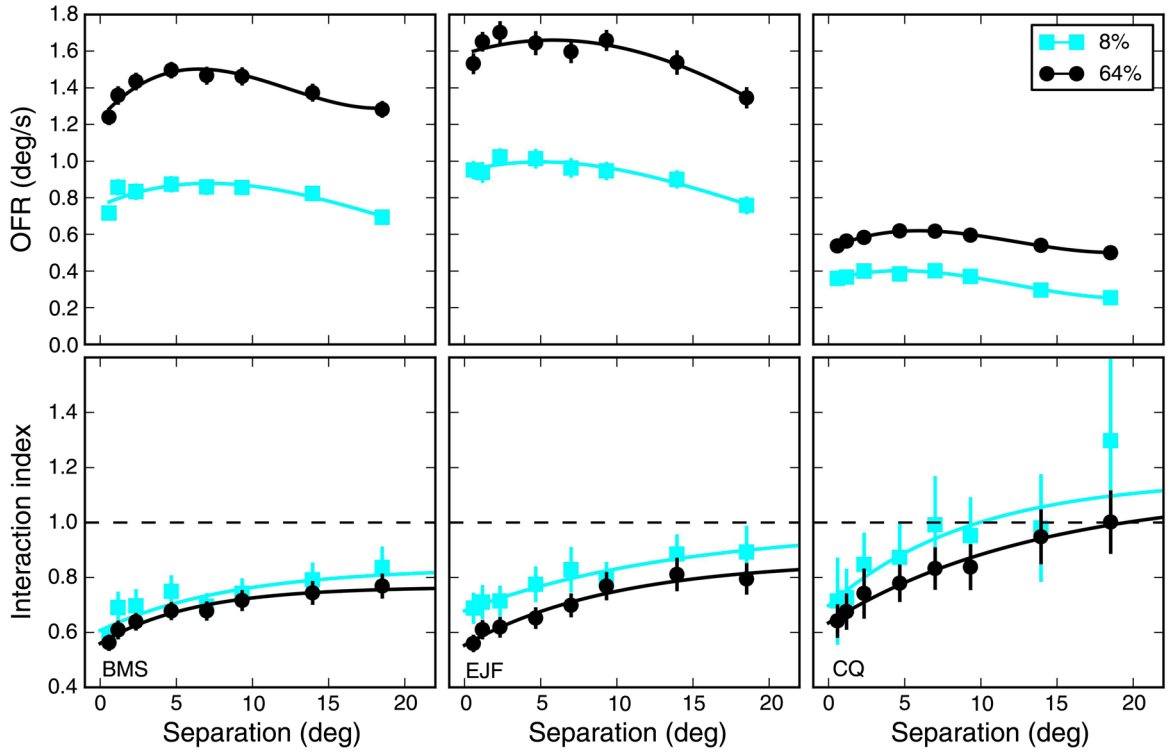

Figure 7.

Spatial properties: contrast dependency. Besides the effect on OFR magnitude just reported (Figure 6), contrast also affects the interaction index. Here we compare responses to 8% and 64% stimuli. The responses to strip pairs (top panels) and the interaction index (bottom panels) are shown, as a function of the separation of the strips. OFRs to strip pairs essentially scaled with contrast. However, contrast did not simply rescale all responses: Lowering the contrast of the stimulus reliably increased the value of I_I, so that suppression observed at high contrast was either reduced or even replaced by facilitation. Error bars indicate ±*SEM*. The responses to strip pairs are fitted with a cubic polynomial, whereas for the interaction index we used the exponential function.

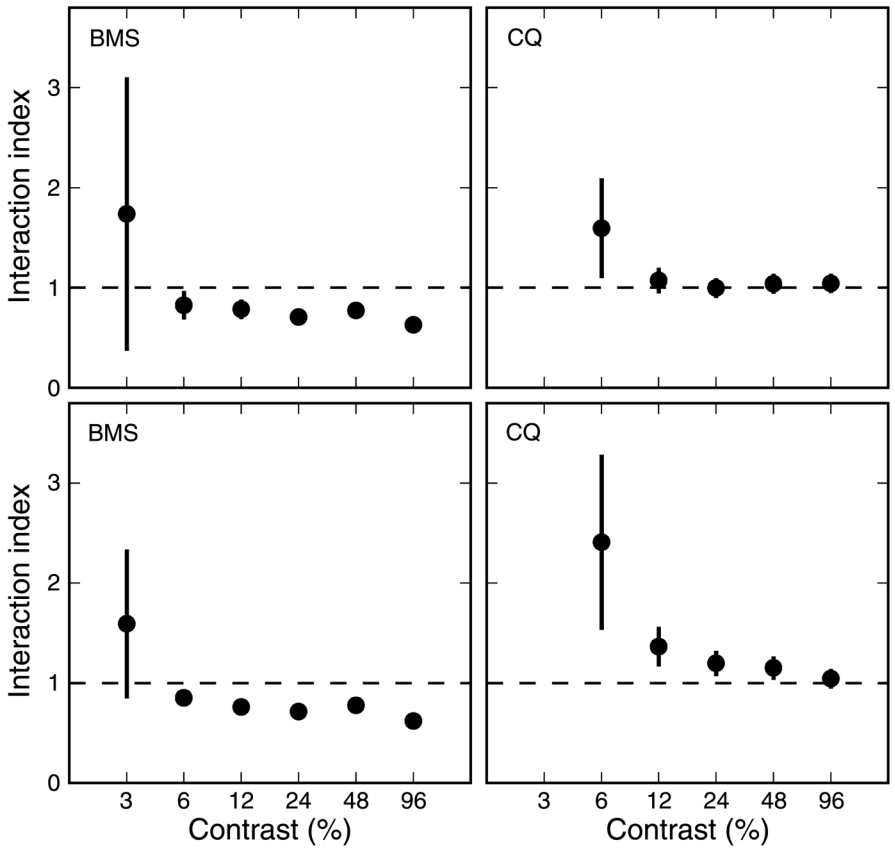

Figure 8.

Interaction index: contrast dependency. To further investigate the effect of contrast, we tested in two subjects the effect on the interaction index (one strip separation only, 14°) of varying contrast between 3% and 96%. Top row: Interaction index as a function of contrast, using stimulus-based measures to compute the OFRs. Bottom row: Same as top row but using pair-based measures. Only at very low contrasts is the effect on the interaction index evident, regardless of the measure used. At these low level, the error bars (±*SEM*) become however quite large.

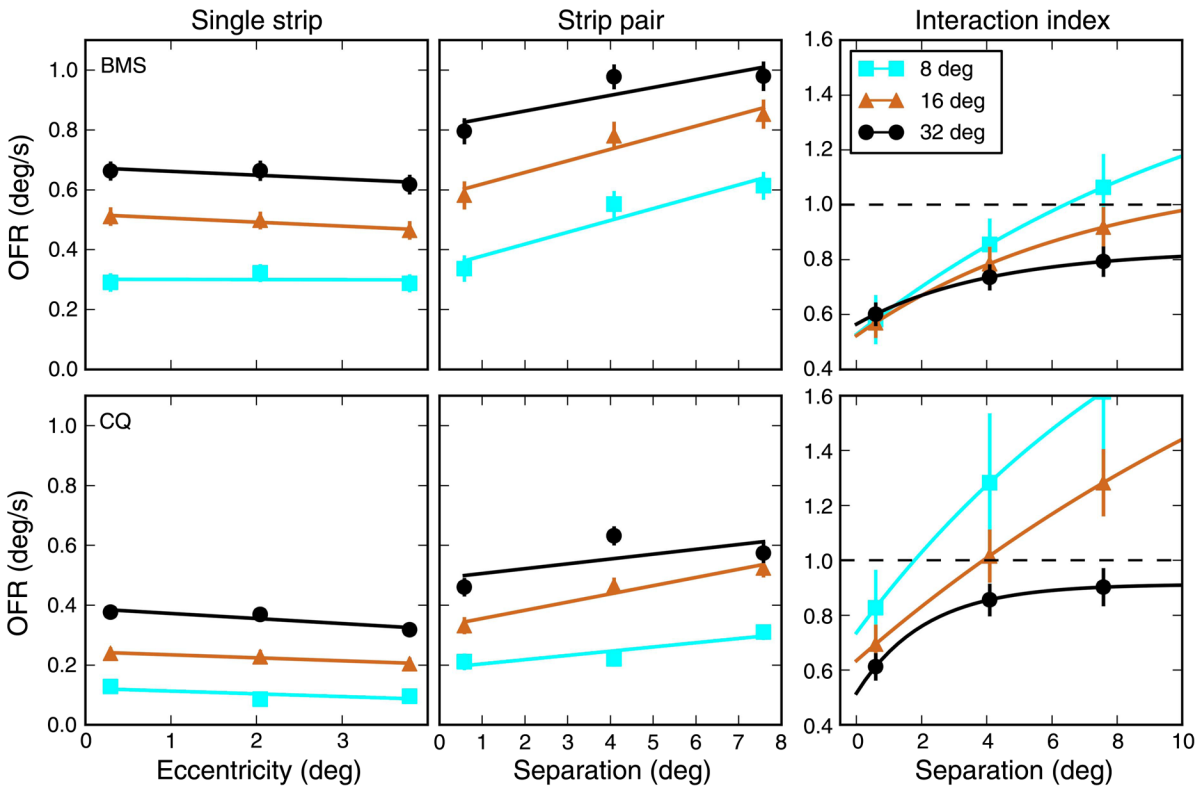

Figure 9.

Effect of strip width. The width of the stimulus strip has a large influence on the magnitude of OFR responses. Both responses to single strip (left column) and to strip pairs (center column) scale with width. The scaling is however not uniform, so that the interaction index (right column) is quite different at the various widths. Because of the reduced magnitude of the responses at the smallest width tested, only very limited eccentricities could be tested. Error bars indicate ±*SEM*. Linear fits were used for single strips and strip pairs; the aforementioned exponential fit was used for the interaction index.

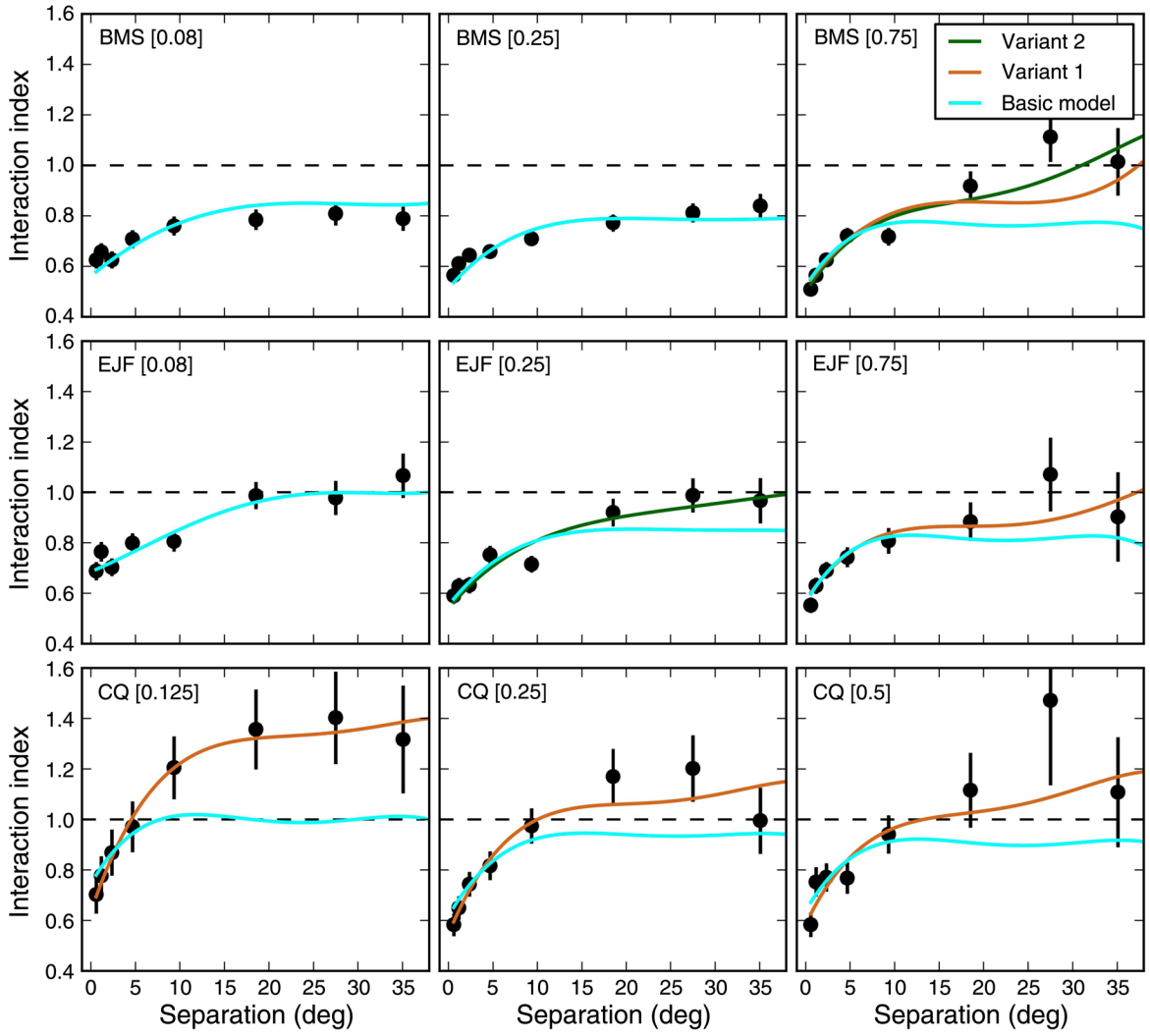

Figure 10.

Model simulations. A very simple model, with only four parameters, is capable of capturing the basic properties of the interaction index (cyan lines). In 5 out of 9 cases, the addition of an output (expansive) non-linearity (variant 1, orange lines) significantly improved the fit. Making the normalization pool local through an additional model parameter (variant 2, green lines) further improved the fits in only two cases. Error bars indicate ±*SEM*. In all cases, the simulations of the best fitting basic model are shown. For the two variants, simulation results are only shown when the improvement over the basic model is significant (χ^2 test increases and AIC decreases). The key in each panel indicates subject and SF.

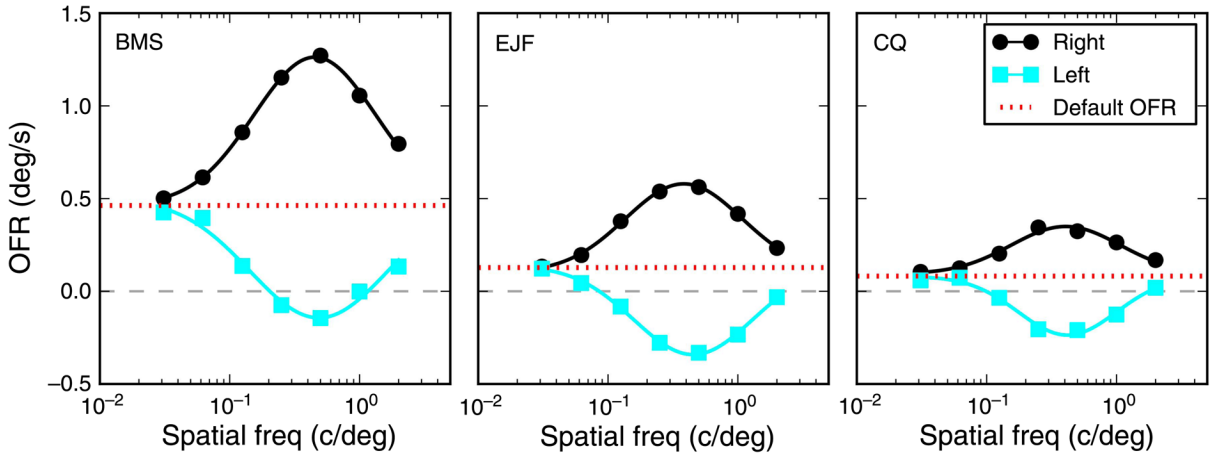

Figure A1.

The OFR default response. While the OFR is generally driven by stimulus motion, the responsiveness of the system extends beyond its selectivity. We measured the OFR of our subjects to a very thin (0.14° high) strip located at eye level, containing gratings of different frequencies. Bars indicating ±*SEM* are plotted as well, but they generally fall within the marker for the mean response. At very high speed (which in our context means very low spatial frequency), the response was the same (red dotted line), and different than zero, whether the stimulus was moving leftward (blue) or rightward (black). The simplest explanation for the smooth transition from selectivity to non-selectivity is that there is a non-selective response superimposed on a selective one. We term this non-selective component the default OFR.

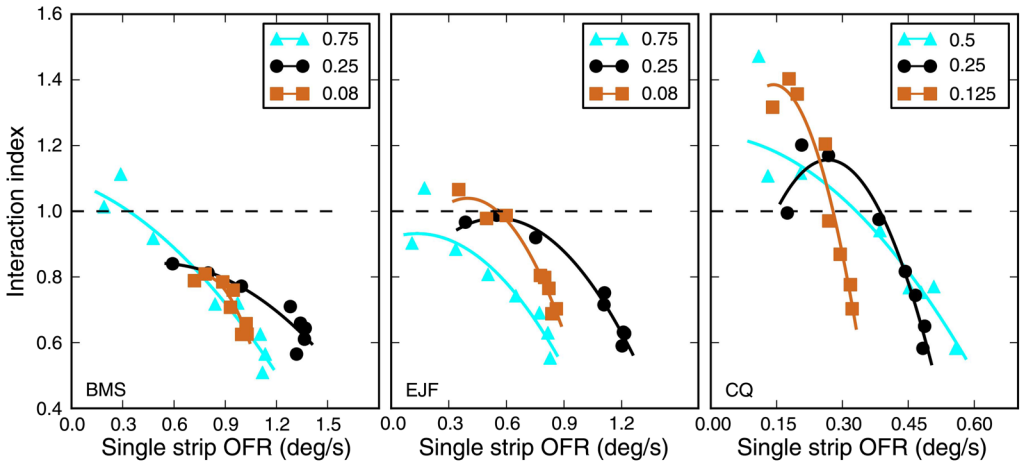

Figure B1.

Interaction index and OFR magnitude are inversely correlated. There is an inverse relationship between the magnitude of the OFR and the interaction index, which we fit, separately for each subject and SF, with a quadratic polynomial using weighted least squares. In principle, this algorithm could not be used, since both the dependent and the independent variables are random variables. However, the variability of the independent variable is much smaller than the range covered, making this algorithm acceptable. For clarity, error bars have been omitted in this plot.

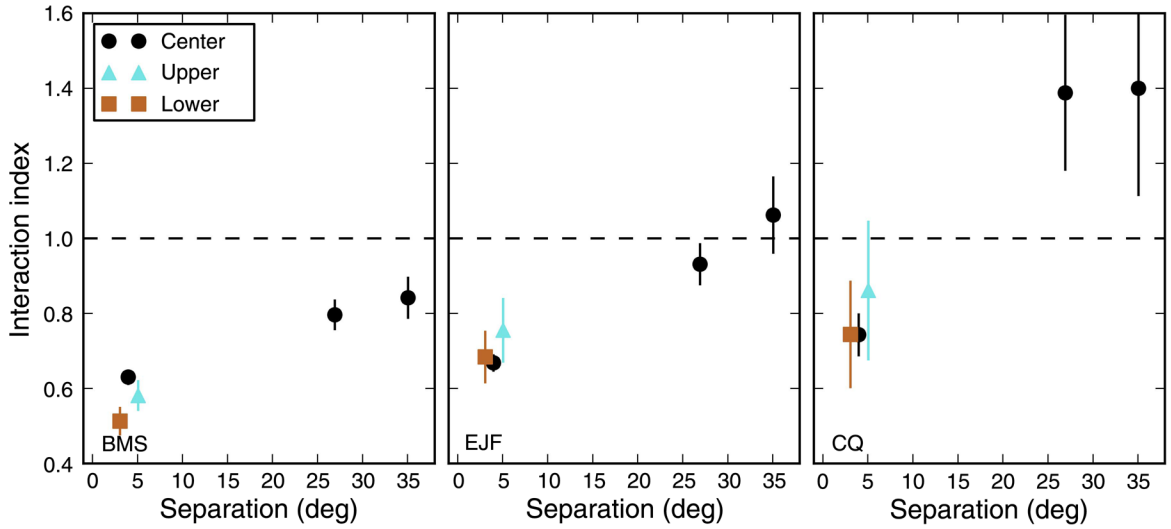

Figure B2.

Strip separation is the main determinant of the interaction index. Same as Figure 5, but now in addition to pairs of strips centered around eye level (black circles), two pairs of strips in the upper and lower peripheries were also presented. This stimulus arrangement dissociated the contribution of strip separation and eccentricity of each strip (and thus magnitude of the OFR response). The three pairs with the same separation (4°; a small horizontal jitter has been added in the plot for clarity) were associated with a very similar I_I, in spite of the vastly different OFRs induced by the single strips. In contrast, far apart pairs were associated with a much higher I_I, in spite of inducing single-strip OFRs similar to those of the peripheral pairs. OFR magnitude thus cannot be the only determinant of the strength of the interaction: Separation must play an important role.

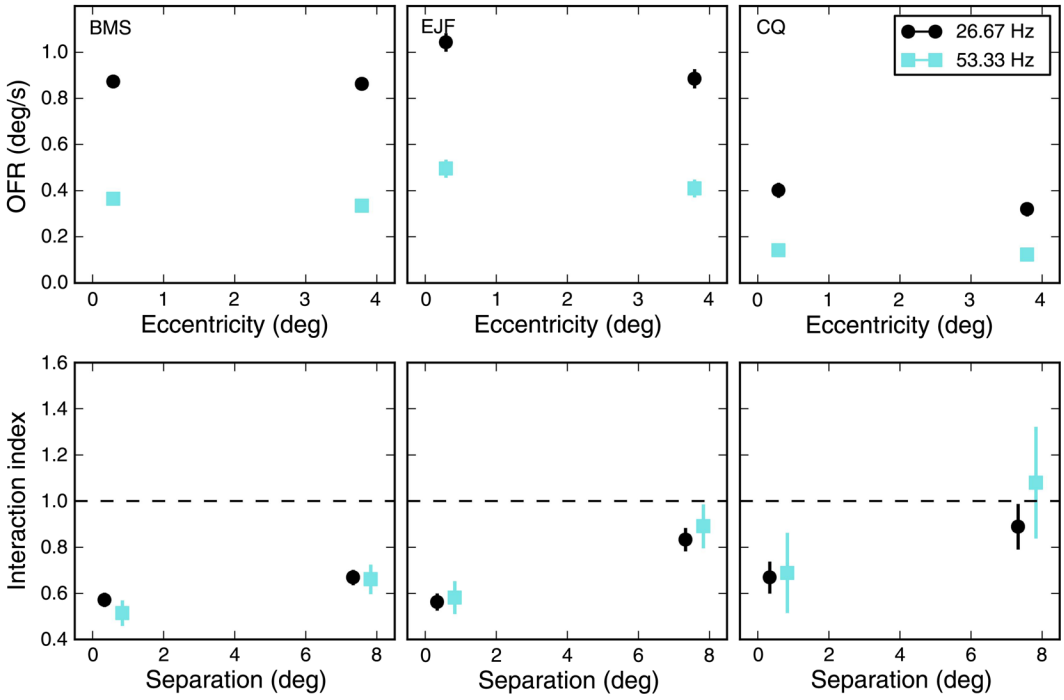

Figure B3.

Interaction index is not affected by temporal frequency. Changing the temporal frequency of the stimulus causes large changes in the magnitude of the OFR to single strips (top row). However, the effect on the interaction index is very limited. OFR magnitude thus cannot play a major role in determining the strength of the interaction, at least over the (rather large) range tested.

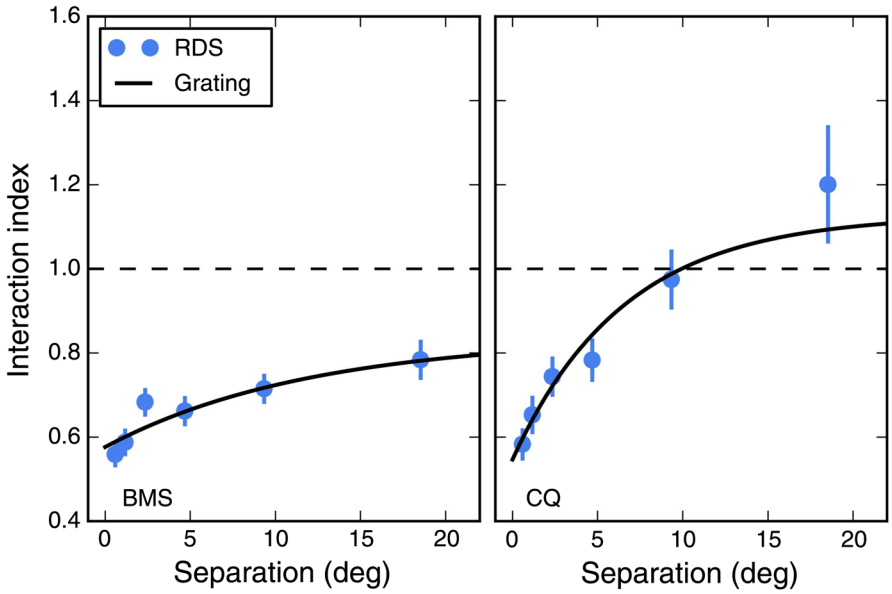

Figure B4.

Interaction index as a function of strip separation for RDS. Strips containing random dots (30% coverage) were presented, either individually or in pairs. As with gratings, when the two strips were close together, they interacted in a strong suppressive manner, so that the response to the strips was only somewhat larger than the response to a single strip. However, when the separation increased the response to the pair became relatively stronger, leading to facilitation at large separation in one of the two subjects. Error bars indicate ±*SEM*. Dashed line indicates linear summation. Here we plot the data from the RDS experiment (blue points) together with the fit to the interaction index from the experiment with sinusoidal (SF = 0.25 cpd) gratings (Figure 5, top row).

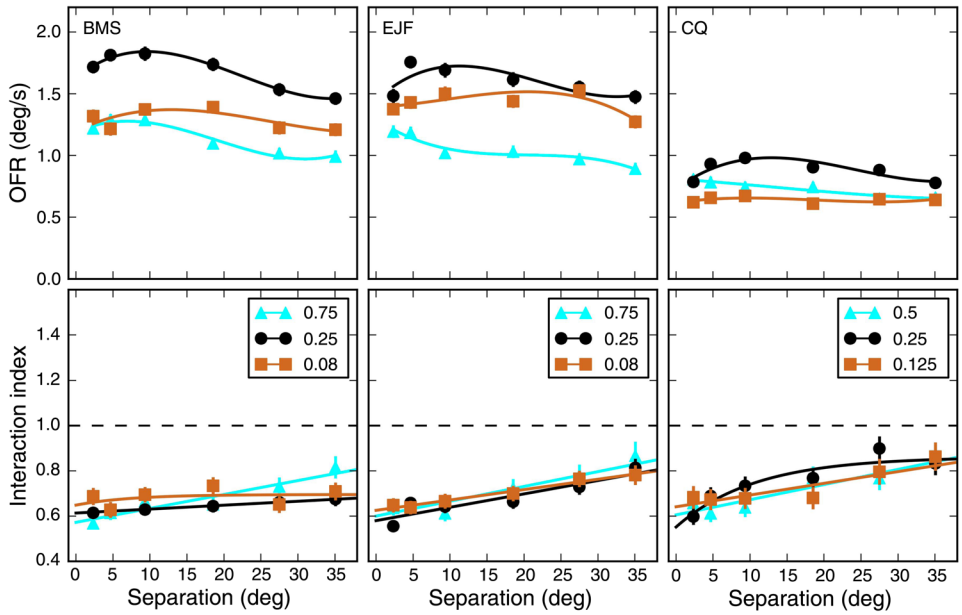

Figure C1.

Response to strip triplets. In a separate experiment, we measured responses to a single strip at eye level, to pairs of strips symmetrically placed around eye level (±1.2°, ±2.3°, ±4.7°, ±9.3°, ±13.7°, and ±17.5°), and to triplets composed of one of the strip pairs together with the central strip. The responses to strip triplets are shown, for our three subjects and for three SFs, in the top panels. Note how the responses modulate much less than when only two strips are used (Figure 3). In the bottom panels, we plot the interaction index, computed as the ratio between the response to each triplet and the sum of the responses to the central strip and to the corresponding strip pair presented alone. Note how the interaction index is low for all separations and does not reach the large values observed with strip pairs (Figure 5, top row). Error bars indicate ±*SEM*. The responses to strip triplets are fitted with a cubic polynomial, whereas for the interaction index we used the exponential function.

Table 1

Model fits for the main experiment.

Subject	SF	τ	σ_e	μ_n	σ_n	G	τ_n	GN_S	GN_P
BMS	0.08	45.0	2.7	19.8	4.6			1.005	1.186
BMS	0.25	20.0	2.0	11.4	6.4			1.191	1.514
BMS	0.75	11.4	1.1	3.5	1.7	1.9	30.9	N/A	N/A
EJF	0.08	16.1	3.5	0.5	1.2			2.0	2.0
EJF	0.25	14.5	2.0	4.0	2.5	8.1	14.9	N/A	N/A
EJF	0.75	9.8	1.0	4.4	3.2	2.6		1.320	1.671
CQ	0.125	34.6	1.8	1.8	5.0	0.2		1.754	1.958
CQ	0.25	23.4	1.5	5.7	5.0	0.3		1.394	1.722
CQ	0.5	11.9	1.4	3.0	1.7	1.2		1.735	1.999